Research Paper

THEMED ISSUE: Anatomy of Rifting: Tectonics and Magmatism in Continental Rifts, Oceanic Spreading Centers, and Transforms

GEOSPHERE

GEOSPHERE; v. 12, no. 6

doi:10.1130/GES01341.1

16 figures; 5 tables; 3 supplemental files

CORRESPONDENCE: a.l.peace@durham.ac.uk

CITATION: Peace, A., McCaffrey, K., Imber, J., Phethean, J., Nowell, G., Gerdes, K., and Dempsey, E., 2016, An evaluation of Mesozoic rift-related magmatism on the margins of the Labrador Sea: Implications for rifting and passive margin asymmetry: Geosphere, v. 12, no. 6, doi:10.1130/GES01341.1.

Received 9 April 2016
Revision received 3 August 2016
Accepted 24 August 2016

An evaluation of Mesozoic rift-related magmatism on the margins of the Labrador Sea: Implications for rifting and passive margin asymmetry

Alexander Peace[1], Ken McCaffrey[1], Jonathan Imber[1], Jordan Phethean[1], Geoff Nowell[1], Keith Gerdes[2], and Edward Dempsey[1]

[1]Department of Earth Sciences, Science Labs, Durham University, Elvet Hill, Durham DH1 3LE, UK
[2]Shell International, 40 Bank Street, London E14 5NR, UK

ABSTRACT

The Labrador Sea is a small (~900 km wide) ocean basin separating southwest Greenland from Labrador, Canada. It opened following a series of rifting events that began as early as the Late Triassic or Jurassic, culminating in a brief period of seafloor spreading commencing by polarity chron 27 (C27; Danian) and ending by C13 (Eocene-Oligocene boundary). Rift-related magmatism has been documented on both conjugate margins of the Labrador Sea. In southwest Greenland this magmatism formed a major coast-parallel dike swarm as well as other smaller dikes and intrusions. Evidence for rift-related magmatism on the conjugate Labrador margin is limited to igneous lithologies found in deep offshore exploration wells, mostly belonging to the Alexis Formation, along with a postulated Early Cretaceous nephelinite dike swarm (ca. 142 Ma) that crops out onshore, near Makkovik, Labrador. Our field observations of this Early Cretaceous nephelinite suite lead us to conclude that the early rift-related magmatism exposed around Makkovik is volumetrically and spatially limited compared to the contemporaneous magmatism on the conjugate southwest Greenland margin. This asymmetry in the spatial extent of the exposed onshore magmatism is consistent with other observations of asymmetry between the conjugate margins of the Labrador Sea, including the total sediment thickness in offshore basins, the crustal structure, and the bathymetric profile of the shelf width. We propose that the magmatic and structural asymmetry observed between these two conjugate margins is consistent with an early rifting phase dominated by simple shear rather than pure shear deformation. In such a setting Labrador would be the lower plate margin to the southwest Greenland upper plate.

INTRODUCTION

Stretching of the continental lithosphere results in rifting and may lead to continental breakup accompanied by seafloor spreading (Eldholm and Sundvor, 1979). The production of pairs of conjugate continental passive margins is the inevitable result of the continental breakup process (Geoffroy, 2005). Although conjugate margins may inherit similar geological and structural components, many aspects of these conjugate pairs often display significant asymmetry.

The degree of symmetry displayed between conjugate passive margins has traditionally been linked to the mode by which the preceding rifting occurred (Lister et al., 1986), with models of continental rifting being described as either pure shear (McKenzie, 1978), simple shear (Wernicke, 1985), or combinations of these (Lister et al., 1986). Rifting under a pure shear–dominated regime occurs by symmetrical, brittle extension of an upper layer and ductile stretching of a lower layer. The simple shear model of rifting predicts that extension occurs along lithosphere-scale normal faults and/or ductile shear zones usually resulting in an asymmetric rift in cross section (e.g., Lister et al., 1986; Etheridge et al., 1989). The large detachment faults required by simple shear models are claimed to be mechanically problematic (Ranero and Pérez-Gussinyé, 2010); it has also been claimed that both conjugate margins often display characteristics of being the upper plate to the detachment fault (Lavier and Manatschal, 2006). It has also been argued that it is difficult to generate melt under simple shear rifting (Latin and White, 1990). Despite these problems, the simple shear model or derivatives of it are often used to explain various aspects of asymmetry on conjugate margin systems, for example, the South Atlantic margins (Becker et al., 2016). Testable predictions of the detachment model of passive margin formation (Lister et al., 1986) include a wide continental shelf, and deep sag basins overlying the sedimentary synrift fill on the lower plate margin. In contrast, the upper plate margin remains relatively unfaulted with an induced continental drainage divide caused by uplift due to magmatic underplating.

In this contribution we assess the degree of asymmetry displayed by the conjugate margins of the Labrador Sea (Fig. 1A) to determine if rifting prior to the formation of these margins is likely to have taken place under a pure or a simple shear–dominated regime. This assessment was achieved through observations made during four weeks of field work between June and July 2015 near the town of Makkovik, Labrador, Canada. The primary aim of the field work was to identify and characterize the spatial extent and field relationships of previously described Mesozoic igneous rocks, which Tappe et al. (2007)

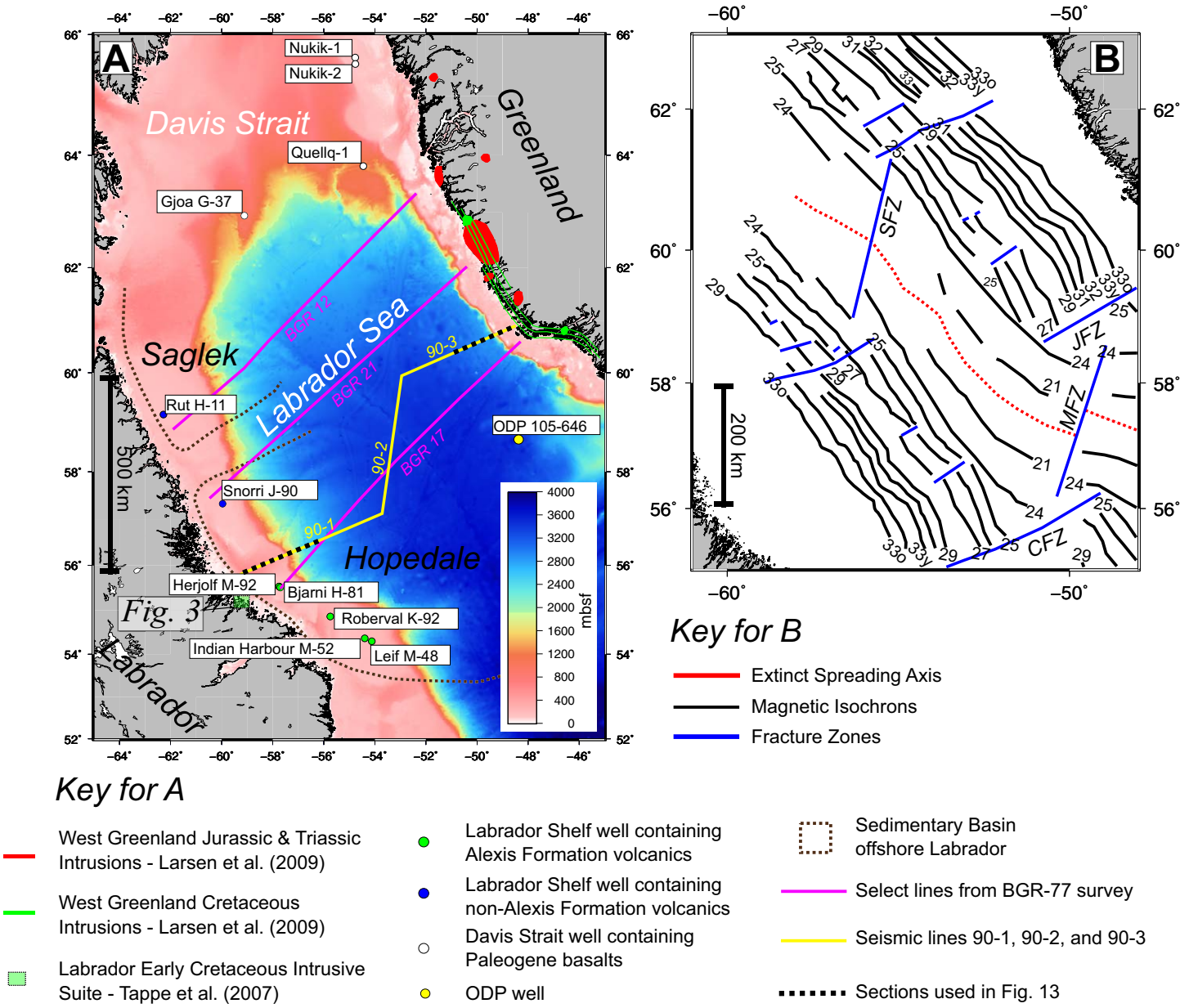

Figure 1. (A) Summary of documented occurrences of early rift-related (Triassic–Cretaceous) magmatism on the margins of the Labrador Sea, both onshore and in offshore wells. ODP—Ocean Drilling Program. (B) Interpretation of the age and structure of oceanic crust in the Labrador Sea (modified from Srivastava and Roest, 1999). Abbreviations: SFZ—Snorri fracture zone; CFZ—Cartwright fracture zone; JFZ—Julinhaab fracture zone; MFZ—Minna fracture zone. The bathymetry data are from Smith and Sandwell (1997; global topography and bathymetry).

related to rifting prior to the opening of the Labrador Sea. Field observations were supplemented by whole-rock geochemistry (X-ray fluorescence, XRF) of igneous rock samples. Our field data are then considered in the context of observations from elsewhere on the margins of the Labrador Sea. We integrate these observations with analysis of large-scale geophysical data sets including that of the National Oceanic and Atmospheric Administration (NOAA; Divins, 2003), seismic reflection profiles, and the Smith and Sandwell (1997) global topography data set to further test our interpretation of margin asymmetry.

GEOLOGICAL SETTING

The Labrador Sea separates Labrador in eastern Canada from southwest Greenland (Fig. 1A) and is floored by a small (~900 km wide) oceanic basin that provides an ideal place to study conjugate passive margin pairs where the production of oceanic crust was relatively limited (Chalmers and Laursen, 1995). Rifting of the Labrador Sea has previously been attributed to either a pure shear–type model, based on seismic and other geophysical data indicating that faulting is confined to the upper crust (Keen et al., 1994), or a simple shear–type model, based on observations of the asymmetry of the transition zones (Chian et al., 1995a).

Rifting prior to the opening of the Labrador Sea started as early as the Late Triassic to Jurassic, based on ages obtained from dike swarms in West Greenland that are interpreted to be related to early rifting (Larsen et al., 2009) (Fig. 1A). The early seafloor spreading history of the Labrador Sea is poorly constrained, with the oldest undisputed magnetic anomaly interpretation in the Labrador Sea being from polarity chron 27 (C27; Danian; Chalmers and Laursen, 1995). However, seafloor spreading may have initiated earlier, at C32 (Campanian) in the southern Labrador Sea and C28 (Maastrichtian) in the northern Labrador Sea (Srivastava, 1978). Seafloor spreading in the Labrador Sea underwent a major reorganization and change in spreading direction at C24–C25N (Thanetian–Ypresian) (Fig. 1B), coincident with the onset of North Atlantic spreading (Srivastava, 1978). After the reorganization of the North Atlantic and Labrador Sea between C24 and C25N there was a reduction in the rate of seafloor spreading before it eventually ceased at C13N (Eocene-Oligocene boundary) (Geoffroy, 2001).

The sedimentary basins offshore Labrador record the progressive opening of the Labrador Sea from south to north (DeSilva, 1999) during the Mesozoic. Two major sedimentary basins are present off the coast of Labrador (DeSilva, 1999): the Hopedale Basin in the south and the Saglek Basin to the north (Fig. 1A). Both the Saglek and Hopedale Basins contain synrift and postrift, clastic-dominated sequences of Cretaceous to Pleistocene age (Jauer et al., 2014). Exposures of Mesozoic and Cenozoic sediments onshore along the Labrador coast are extremely rare (Haggart, 2014).

From north to south the basement tectonic units exposed at surface on the coast of Labrador are the Archean Nain Province, the Paleoproterozoic Makkovik Province, and the Mesoproterozoic Grenville Province (LaFlamme et al., 2013; Fig. 2). The Makkovik Province is separated from the Nain Province by the Kanairiktok shear zone (Culshaw et al., 2000) and from the Grenville Province by the Grenville Front, which marks the northern limit of widespread Grenvillian deformation (Funck et al., 2001). The Makkovik Province is characterized as a Paleoproterozoic accretionary belt and is the smallest defined tectonic component of the Canadian shield (Ketchum et al., 2002). Prior to the opening of the Labrador Sea the Makkovik Province was adjacent to the Ketilidian mobile belt (KMB; Fig. 2), which currently forms part of southwest Greenland (e.g., Garde et al., 2002; Wardle et al., 2002; Kerr et al., 1997). The Makkovik Province can be separated into three distinct zones with distinctive geological characteristics (Kerr et al., 1996); from northwest to southeast, they are the Kaipokok, Aillik, and Cape Harrison domains (Fig. 2) (Kerr et al., 1997).

Onshore Rift-Related Magmatism on the Margins of the Labrador Sea

Our field work was carried out in the Aillik domain of the Makkovik Province. Here, the Early Cretaceous nephelinite suite (ca. 142 Ma) located near Makkovik (Fig. 3; Table 1) is the most recent of three magmatic events identified by Tappe et al. (2007). The older two magmatic events formed a Neoproterozoic ultramafic lamprophyre and carbonatite dike suite (ca. 590–555 Ma) and a Mesoproterozoic olivine lamproite dike suite (ca. 1374 Ma) (Tappe et al., 2006). These two older events are not considered to be directly related to the rifting that culminated in the Mesozoic opening of the Labrador Sea (Tappe et al., 2007).

The Tappe et al. (2007) nephelinite suite (Fig. 3; Table 1) comprises fine-grained olivine melilitite, nephelinite, and basanite dikes and sills as much as 2 m thick with a preferential east-west orientation, and has been characterized as a type of rift-related magmatism. This intrusive suite was claimed by Tappe et al. (2007) to be analogous to the coast-parallel alkaline basaltic dikes observed between 60° and 63°N in West Greenland (Larsen, 2006). The samples categorized by Tappe et al. (2007) as belonging to the nephelinite suite are summarized in Table 1, along with their relationship to the samples collected and our analyses (described herein). Here we use the definition of Le Bas (1989) of a nephelinite as containing >20% normative nepheline.

Magmatism in West Greenland has also been attributed to early rifting, prior to the opening of the Labrador Sea. According to Larsen et al. (2009) this magmatism is manifest as Mesozoic–Paleogene intrusive rocks that range in scale and abundance from large, coast-parallel dike swarms to small, poorly exposed dike swarms or single intrusions (Fig. 1; Table 2). The large coast-parallel dikes extend for 380 km along the southwest Greenland coast (Larsen et al., 1999). Chalmers et al. (1995) described the later Paleogene breakup-related flood basalts farther north in and around the Davis Strait, but these are beyond the geographical and temporal scope of this study. The igneous rocks observed onshore southwest Greenland (Table 2) demonstrate that multiple magmatic events occurred on this margin during and after the Mesozoic. Although many of these events are likely to be rift related, it is extremely unlikely that all these igneous rocks were produced due to the same event.

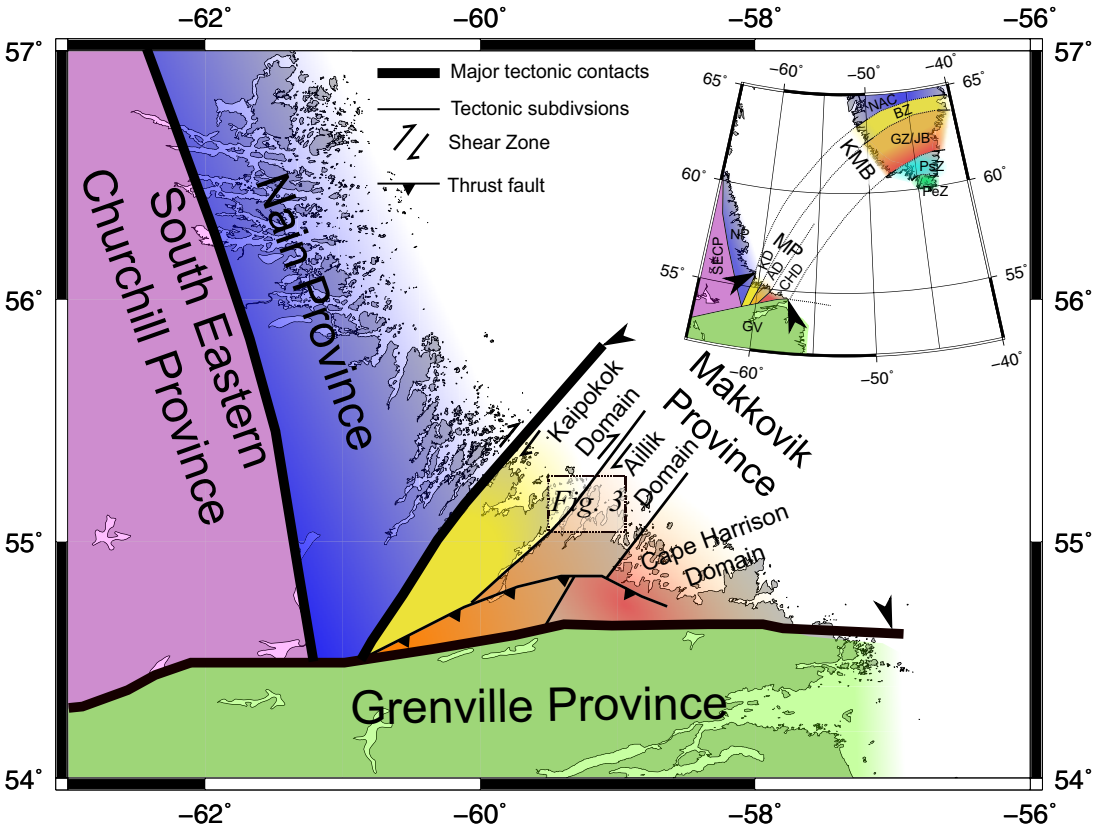

Figure 2. Simplified tectonic framework of central Labrador modified from LaFlamme et al. (2013), including the location of Figure 3 within the Makkovik Province. Abbreviations: NAC—North Atlantic Craton; BZ—Border Zone; GZ/JB—Granite Zone/Julianehåb Batholith; NP—Nain Province; MP—Makkovik Province; PsZ—Psammite Zone; PeZ—Peliet Zone; SECP—southeastern Churchill Province; KD—Kaipokok Domain; AD—Ailik Domain; GV—Grenville Province; KMB—Ketilidian Mobile Belt. Inset: The correlation of the Makkovik and Ketilidian orogenic belts modified from Kerr et al. (1997).

Offshore Rift-Related Magmatism on the Margins of the Labrador Sea

Mesozoic magmatism has also been observed and documented in exploration wells on the Labrador shelf (Fig. 1A; Table 3) (Umpleby, 1979). Volcanic rocks that are believed to have been erupted during the early stages of rifting are mostly assigned to the Alexis Formation; the type section is recorded in the Bjarni H-81 well (e.g., Ainsworth et al., 2014; Umpleby, 1979). Here a sequence of basalts interspersed with sandstones and silty clays was recorded, but no pyroclastic rocks were documented (Umpleby, 1979). Two cores from the Alexis Formation in Bjarni H-81 have been dated using K-Ar bulk-rock analysis. The lowermost core came from 2510 m and basaltic rocks have been dated as 139 ± 7 Ma (Valanginian), while those in the upper core at 2260 m were dated as 122 ± 6 Ma (Aptian). The age of the lower core is deemed to be less reliable due to alteration; Umpleby (1979) suggested that the inferred duration of ~17 m.y. for the magmatic event resulting in the eruption of the Alexis Formation is too long and that the lower core might be younger.

The total thickness and areal extent of the basalts of the Alexis Formation is not well constrained, beyond the occurrence of volcanic rocks in the Leif M-48, Robertval K-92, Bjarni H-81, Indian Harbour M-52, and Herjolf M-92 wells (Fig. 1A and Table 3). The Alexis Formation occurs in the Hopedale Basin (Hamilton and Harrison subbasins) and within the southern part of the Saglek Basin, but has not been recorded in the more northern Nain subbasin within the Hopedale Basin (Ainsworth et al., 2014). The thickest recorded occurrence of the Alexis Formation is 357 m in the Robertval K-92 well (Ainsworth et al., 2014). Note that some igneous rocks intersected by wells on the Labrador Shelf have not been assigned to a formation (Ainsworth et al., 2014). Occurrences of unclassified igneous rocks include the "Tuff" and "Diabase" intervals (Canada-Newfoundland and Labrador Offshore Petroleum Board, 2007) in Rut H-11 and the sediments derived from volcanic material in Snorri J-90 (McWhae et al., 1980).

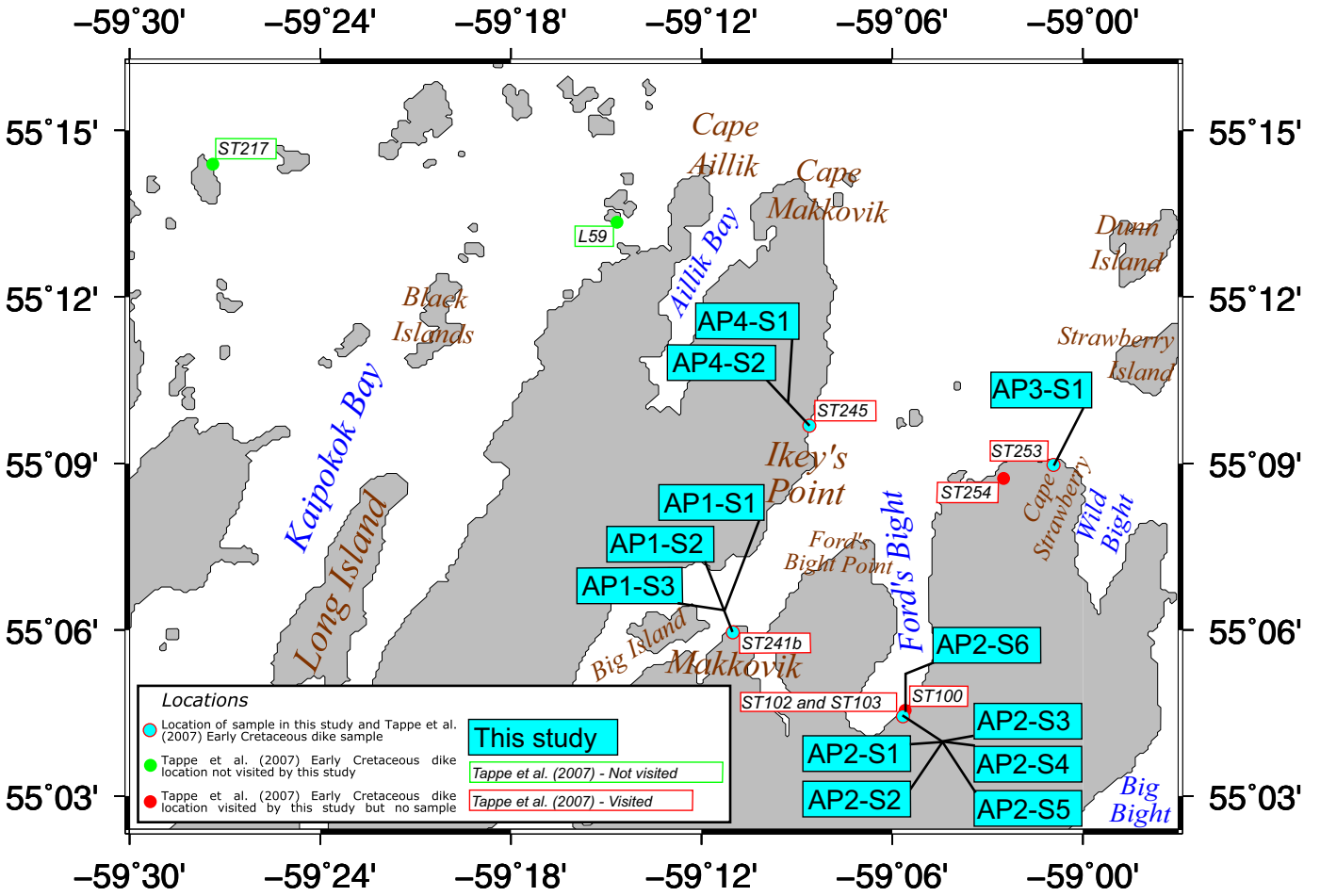

Figure 3. Map of the area surrounding Makkovik. Blue filled boxes depict the samples collected and analyzed in this study. The Tappe et al. (2007) samples are depicted as smaller red and green boxes, for sites visited and not visited by this study, respectively.

TABLE 1. SUMMARY OF RELATIONSHIP BETWEEN EARLY CRETACEOUS NEPHELINITE SUITE SAMPLES OF TAPPE ET AL. (2007) AND SAMPLES COLLECTED FOR THIS WORK

Tappe et al. (2007) sample number	ST100	ST102	ST241b	L59	ST217	ST103	ST253	ST245	ST254
Composition (Tappe et al., 2007)	Nephelinite	Basanite	Nephelinite	Nephelinite	Basanite	Melilitite	Nephelinite	Basanite	Nephelinite
Samples collected by this work (AP)	No in situ outcrop at location	No in situ outcrop at location	AP1-S1 AP1-S2 AP1-S3	Not visited in our study	Not visited in our study	AP2-S1 AP2-S2	AP3-S1	AP4-S1 AP4-S2	Area of basement exposure but no dikes of any age anywhere in proximity to location.
Coordinates of samples collected by this work (WGS84)	n/a	n/a	55.09927N 59.18356W	n/a	n/a	55.07389N 59.09430W	55.14959N 59.01542W	55.16138N 59.14338W	n/a

Note: WGS84—World Geodetic System 1984. n/a—not applicable as no equivalent sample was obtained by this work.

TABLE 2. DOCUMENTED OCCURANCES OF RIFT-RELATED MAGMATISM IN SOUTHWEST GREENLAND

Locality	Character	Rock type	Method	Age (Ma)	Reference
Uummannaq Fjord	Few small dikes	ailikite	Rb-Sr	186	Larsen et al. (2009)
Ubekendt Ejland	Small dike swarm	camptonite, monchiquite	$^{40}Ar/^{39}Ar$	34 ± 0.2	Storey et al. (1998)
Southeast Nuussuaq	Dikes and sill, some large	tholeiitic basalt	$^{40}Ar/^{39}Ar$	56.8 ± 0.2	Larsen et al. (2009)
West of Disko	Volcanic neck	alkali basalt	$^{40}Ar/^{39}Ar$	27.8 ± 0.6	Storey et al. (1998)
Western Disko	Regional dike swarm	tholeiitic basalt	$^{40}Ar/^{39}Ar$	54.3 ± 0.3	Storey et al. (1998)
Aasiaat district	Three large dikes , one sill	tholeiitic basalt	$^{40}Ar/^{39}Ar$	56, 61	Larsen et al. (2009)
Itilleq	One dike	tholeiitic basalt	$^{40}Ar/^{39}Ar$	64 ± 1.3	Larsen et al. (2009)
Qaqqarsuk	Central complex and dikes	carbonatite, aillikite	Rb-Sr U-Pb*	ca. 165	Secher et al. (2009)
Fossilik	One explosion breccia	ailikite	Rb-Sr	164.2 ± 1.8	Secher et al. (2009)
Søndre Isortoq	Small dike swarm	camptonite, one alkali basalt	$^{40}Ar/^{39}Ar$	56, 58	Larsen et al. (2009)
Godthåbsfjord	Scattered dikes	camptonite	$^{40}Ar/^{39}Ar$	51.8 ± 0.9	Larsen et al. (2009)
Tikiusaaq	Central complex and dikes	carbonatite and aillikite	Rb-Sr U-Pb*	165–155	Tappe et al. (2009)
Færingehavn	Few dikes	aillikite	Rb-Sr U-Pb	159 223	Larsen et al. (2009)
Frederikshåb Isblink	One large dike	phonolite	$^{40}Ar/^{39}Ar$	106.1 ± 1.5	Larsen et al. (2009)
Frederikshåb Isblink	Loose dike swarm	monchiquite, alnöite, carbonatite	Rb-Sr U-Pb*	152–149	Larsen et al. (2009)
Paamiut	Small dike swarm	aillikite	K-Ar	166 ± 5	Larsen and Møller (1968)
Pyramidefjeld	Small dikes and sills, including a thick sheet on Midternæs (16 km NNE)	aillikite	U-Pb	152–150	Frei et al. (2008) Larsen et al. (2009)
Southwest Greenland	Large regional dike swarm	mildly alkaline basalt	$^{40}Ar/^{39}Ar$	141–133	Larsen et al. (1999) Larsen et al. (2009)
Tuttutooq	One or a few sills	camptonite	$^{40}Ar/^{39}Ar$	115.4 ± 4.7	Larsen et al. (2009)

Note: A summary from north to south of documented intrusive rift-related magmatism in West Greenland as summarized by Larsen et al. (2009).
*Samples dated by Rb-Sr or U-Pb on phlogopite or perovskite.

[1]Supplemental Materials 1. Detailed descriptions of all samples mentioned in the manuscript. Please visit http://dx.doi.org/10.1130/GES01341.S1 or the full-text article on www.gsapubs.org to view Supplemental Materials 1.

[2]Supplemental Materials 2. Sample locations and coordinate systems. Please visit http://dx.doi.org/10.1130/GES01341.S2 or the full-text article on www.gsapubs.org to view Supplemental Materials 2.

Although no exploration wells have been drilled on the continental shelf offshore southwest Greenland, Site 646 (Leg 105 of the Ocean Drilling Program, ODP) was drilled on oceanic crust in the southern Labrador Sea (Fig. 1A). With the exception of the oceanic crust, Site 646 did not encounter igneous rocks; however, sediments containing clasts of mafic material were described (Shipboard Scientific Party, 1987).

FIELD OBSERVATIONS OF MESOZOIC MAGMATISM NEAR MAKKOVIK, LABRADOR

The aim of the field work was to characterize the nature and extent of Mesozoic magmatism near Makkovik to gain insights into rifting in the region prior to the opening of the Labrador Sea. Our field study of the Mesozoic magmatism near Makkovik was guided by the description of the Early Cretaceous magmatism in Tappe et al. (2007) (Fig. 3; Table 1). Of the nine locations where Tappe et al. (2007) documented Early Cretaceous magmatism, we visited seven sample locations (with exception of L59 and ST217). Eight samples of igneous material were obtained at four of the seven locations visited during this study. Where appropriate, samples collected adjacent to the dikes are also described to provide geological context and to emphasize the field relationships observed for the dikes.

At three of the Tappe et al. (2007) sample locations (ST100, ST102, and ST245; Fig. 3) we were unable to locate the in situ dikes reported by them. Descriptions including mineralogy, texture, and orientation of all the samples are available in the supplemental data (Supplemental Materials 1[1]). Details of the locations, coordinate systems, and the relationship between samples in this work and Tappe et al. (2007) are also available in the supplemental data (Supplemental Materials 2[2]).

Sample Locations, Field Relationships, and Structural Analysis

Makkovik Peninsula

The three samples with the prefix AP1 represent the three dikes found on the peninsula north of the town of Makkovik (Fig. 3), locally referred to as the Hill. The outcrops from which these samples were obtained are on the southern end

TABLE 3. OCCURRENCES OF VOLCANIC ROCKS IN OFFSHORE WELLS ON THE LABRADOR SHELF

Well name	Depths of igneous rocks	Dating method	Age	Description and Interpretation of igneous rocks
Bjarni H-81	2255 m–total depth	K-Ar	139 ± 7 Ma for the lower core (2510 m) 122 ± 6 Ma for the upper core (2260 m)	Basalts interspersed with sandstones and silty clays, with no pyroclastic rocks. Bjarni H-81 is the type section of the Alexis Formation.
Leif M-48	1839 m–total depth	K-Ar	104 ± 5 Ma to 131 ± 6 Ma	The Leif Basalts are deemed to be coeval and lithologically similar to those in Bjarni H-81, and thus can be considered part of the Alexis Formation.
Indian Harbour M-52	3250 m–3484 m	K-Ar	90 ± 4 Ma for rock fragments (exact stratigraphic position unknown)	The recovered rock samples are lapilli tuff deposits. The volcanic rocks in this well are noted as being lithologically very different from occurrences of the Alexis Formation elsewhere on the Labrador shelf. The lithological difference along with the younger age suggests that these rocks may not be part of the Alexis Formation.
Herjolf M-92	3751 m–4048 m	K-Ar	The top of the volcanic section has been dated as 122 ± 2 Ma, whereas the bottom is dated as 314 ± 12 Ma. This bottom section is severely altered and thus the age is likely to be unreliable.	Subaerial weathered basalt flows overlying Precambrian basement. Lithologically similar to the igneous rocks in Bjarni H-81, and thus can be considered part of the Alexis Formation.
Roberval K-92	3188 m–3544 m	n/a	undated	This is the thickest recorded section of the Alexis Formation (Ainsworth et al., 2014).
Rut H-11	Tuff top at 4432 m and “Diabase intrusive” 4451 m C-NLOPB (2007)	n/a	undated	Igneous rocks are noted twice in the Canada-Newfoundland and Labrador Offshore Petroleum Board (2007) report: Tuff top at 4432 m and “Diabase intrusive” at 4451 m.
*Snorri J-90	3150 m–3061 m (Umpleby, 1979)	palynology	Valanginian to Barremian	A series of graywackes, sands, silts, and coal beds interpreted to be derived from volcanic rocks that may be coeval with the Alexis Formation but should not be referred to as part of the Alexis Formation (McWhae et al., 1980).

Note: Summary of occurrences of volcanic rocks in offshore wells on the Labrador shelf well depths are from C-NLOPB (2007); all other data and information are from Umpleby (1979) and references therein, unless otherwise stated.
*Indicates the presence of sediments potentially derived from igneous rocks. n/a—not applicable as the sample has not been dated.

of a beach (Fig. 4) that marks the intersection between a large linear gully that extends 1 km inland on a bearing of 198°, and the western coast of the peninsula. The dikes that provided samples AP1-S1 and AP1-S2 are well exposed, but the dike from which AP1-S3 was collected is only fully exposed during low tide.

AP1-S1 and AP1-S2 were collected from two different parallel dikes in an approximately north-south orientation (Fig. 4), and are ~1 m and ~2 m thick, respectively. The dike that provided sample AP1-S3 is oriented approximately east-west and is much smaller than the north-south dikes, being only ~30 cm wide. The dike from which AP1-S3 was obtained is crosscut by the dike from which AP1-S2 was obtained. The age relationship between AP1-S1 and AP1-S2 could not be determined from field relationships.

Ford's Bight

Ford's Bight is the elongate bay between Ford's Bight Point and Cape Strawberry, where three of the nine occurrences of Early Cretaceous magmatism reported by Tappe et al. (2007) are located (Fig. 3). Samples in this study with the prefix AP2 were collected at the Tappe et al. (2007) location ST103 on the eastern side of Ford's Bight (Figs. 3 and 5A), with the exception of AP2-S6, which was collected 45 m away from AP2 on a bearing of 025° (Fig. 5B). At the location of AP2 (Fig. 5B), a poorly exposed outcrop within the intertidal range (Figs. 5C, 5D) contained two dikes (sites of samples AP2-S1 and AP2-S2), within a diatreme breccia (samples AP2-S5 and AP2-S6) in proximity to exposed metamorphosed basement (samples AP2-S3 and AP2-S4) (Fig. 5C). An overview of the spatial relationship between the lithologies at AP2 is provided in Figures 5B and 5C. Although we visited sites ST100, ST102, and ST103 (Fig. 5A) during our field study, no in situ outcrop was found at ST100 and ST102; however, small boulders, as wide as 1 m, of the breccia material similar to that observed in samples AP2-S5 and AP2-S6 were observed at these locations.

The dike from which sample AP2-S1 (Fig. 5) was collected (dike 1) is oriented approximately north-south, whereas the dike from which sample AP2-S2 was obtained (dike 2) is oriented approximately east-west. Both dikes vary in thickness along their observable length; dike 1 varies in thickness from 25 to 40 cm and dike 2 varies from 20 to 30 cm. At the AP2 location it was observed that dike 2 crosscuts dike 1, and thus the east-west–oriented dike 2 is younger.

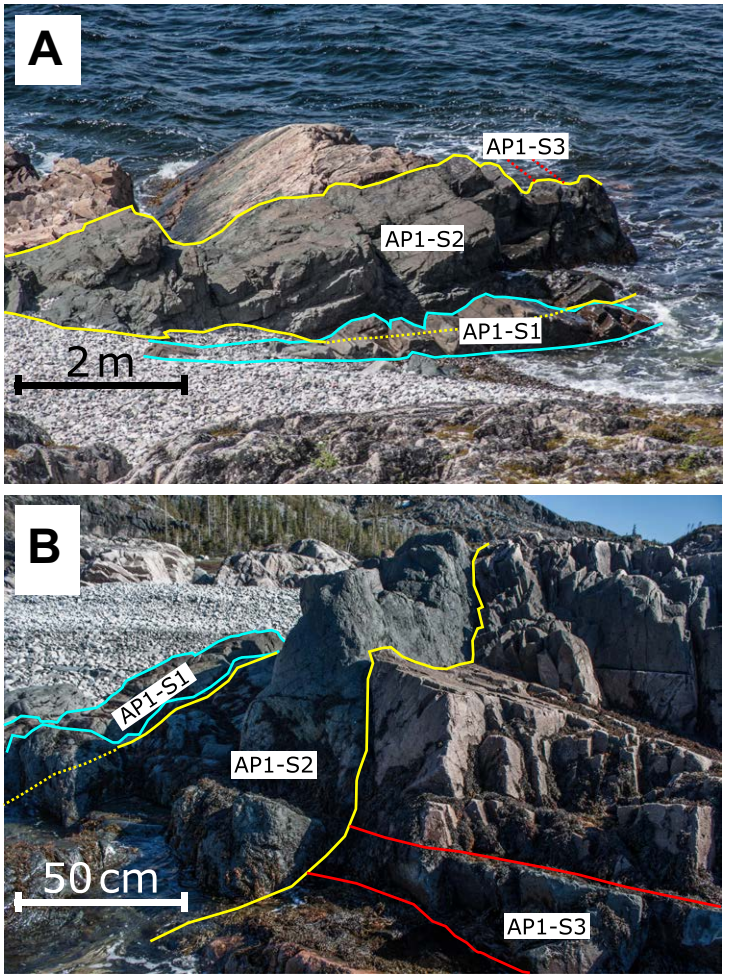

Figure 4. (A) Looking west onto the location AP1 in which three dike samples were analyzed during the study (AP1-S1, AP1-S2, AP1-S3). (B) Looking southeast.

Cape Strawberry

Cape Strawberry is a large headland between Ford's Bight and Big Bight to the northeast of Makkovik. Tappe et al. (2007) described Early Cretaceous magmatism on Cape Strawberry at two locations (ST254 and ST253; Fig. 3). We collected sample AP3-S1 in proximity to ST253 (Fig. 6). ST254 is the location of the only sample in the Early Cretaceous suite that was been dated by $^{40}Ar/^{39}Ar$ methods (141.6 ± 1.0 Ma) by Tappe et al. (2007), and it is also the only location situated inland (Fig. 3). While it is an area of relatively good exposure (Fig. 7) of the 1720 Ma Cape Strawberry Granite (Hinchey, 2013), no nephelinite dikes were observed at this location or anywhere in the vicinity. Thus we were unable to establish field relationships or acquire an equivalent sample for further analysis.

North of Ikey's Point

Ikey's Point is located on the southeastern side of the large peninsula north of Makkovik (Fig. 3). Two dike samples were collected from the area north of Ikey's Point, at the site of previously reported Mesozoic magmatism, and are denoted with the prefix AP4 (Fig. 8). Sample AP4-S1 was collected ~15 m south of ST245, and sample AP4-S2 was collected on a separate dike a further 5 m south of AP4-S1.

Samples AP4-S1 and AP4-S2 are both oriented approximately east-west and display multiple bridge structures (Fig. 8C). The dikes are <13 cm and 25 cm thick for AP4-S1 and AP4-S2, respectively. No crosscutting relationships were observed between AP4-S1 and AP4-S2, thus relative ages could not be determined for the AP4 dikes.

Structural Analysis

An overview of the orientations of the dikes sampled during this study is provided in Figure 9. AP3-S1 is not included in Figure 9 because this sample was obtained from a boulder (Fig. 6B). Figure 9A demonstrates that the dikes sampled by this study do not appear to be part of a singular, systematic dike swarm. Figure 9B demonstrates that none of the dikes analyzed during our study at locations where Mesozoic magmatism has been documented previously are margin parallel, i.e., striking 130°–150°. Margin-parallel orientations might be the predominant trend expected for dikes intruded during rifting, unless a stress reorientation occurred at the rift margin (e.g., Philippon et al., 2015).

Lithological Descriptions and XRF Analysis

In the following section lithologies are described and the results of XRF analysis (Supplemental Materials 3[3]) on the samples obtained by this study are presented. Thin sections in both plane and cross-polarized light are presented in Figure 10; full descriptions to complement those given in this section are provided in the Supplemental Materials 1 (see footnote 1).

Makkovik Peninsula

The gray dike from which sample AP1-S1 was obtained has an extremely fine-grained groundmass that surrounds a main phenocryst phase of clinopyroxene (60%), which is generally arranged into star-shaped clusters of two or more crystals. Highly altered olivine (15%) is also present, along with apatite (<5%), amphibole (<5%), and biotite (<5%). Some vesicles infilled with calcite were as much as 6 mm wide, but most were ~2 mm wide.

Supplementary information 3: XRF analysis and datasets

XRF (X-ray fluorescence) major element analysis was undertaken at the University of Leicester, UK to determine the weight percent of major elements as oxides. The XRF laboratory at the University of Leicester operates a PANalytical Axios Advanced X-Ray Fluoresence spectrometer which runs a 4Kw Rhodium (Rh) anode end window super sharp ceramic technology X-Ray tube. The major element analysis was performed on fused beads to eliminate mineralogical effects and reduce inter-element effects.

Other datasets used by this study include: the NOAA total sediment thickness data Version 2 (Whittaker et al., 2013); and Smith and Sandwell global topography and Bathymetry Version 18.1 (Smith and Sandwell, 1997). Our investigation into offshore sediment distribution utilises Version 2 of the NOAA total sediment thickness dataset despite the update of the original only applying to the Australia-Antarctic region as this was the latest version available at the time of this work. The NOAA total sediment thickness dataset has a grid resolution of five by five arc-minutes, with the data contributing to this dataset obtained from sources including; previously published isopach maps, ocean drilling results and seismic reflection profiles. Version 18.1 of the global topography and bathymetry data (Smith and Sandwell, 1997) dataset is primarily sourced from multibeam cruise data, supplemented by Version 23 (Sandwell et al., 2014) of the satellite derived free air gravity.

[3]Supplemental Materials 3. X-Ray Fluorescence analysis and other datasets. Please visit http://dx.doi.org/10.1130/GES01341.S3 or the full-text article on www.gsapubs.org to view Supplemental Materials 3.

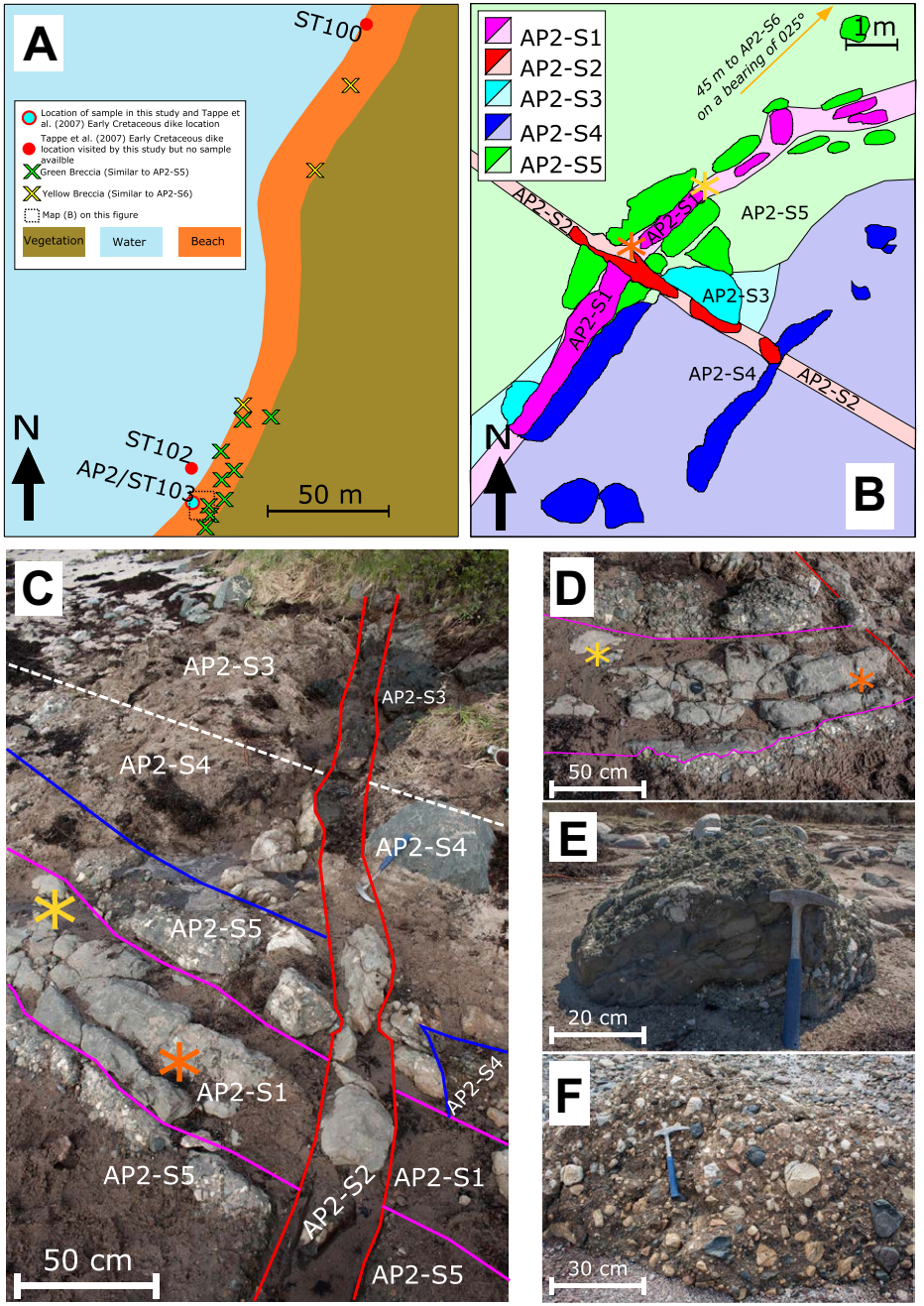

Figure 5. (A) An overview of occurrences of diatreme breccia in Ford's Bight along with the locations of samples collected during this study and Tappe et al. (2007). For the location of the samples on this inset within Ford's Bight, see Figure 3. Differentiation is made between a green diatreme breccia that resembles AP2-S5 (green cross) and one that is more yellow in color, similar to AP2-S6 (yellow cross). Many of the occurrences shown are not in situ. (B) The spatial relationship between the different lithologies described at AP2. (C) Looking southeast onto the two small (<50 cm) crosscutting melilitite dikes (samples AP2-S1 and AP2-S2) within the Ford's Bight diatreme. (D) The contact between dike 1 (sample AP1-S1) and the surrounding diatreme breccia (sample AP2-S5) looking toward the south. (E) Boulder on the beach in Ford's Bight looking west comprising green diatreme breccia (similar to AP2-S5) but with an exceptionally large inclusion of mafic igneous material. (F) Possible in situ outcrop similar to sample AP2-S6 in Ford's Bight looking west. In C and D, purple and red outlines are used to denote the contacts of the dikes from which the samples AP2-S1 and AP2-S2, respectively, were obtained with the breccia and the metamorphosed basement. The blue line in C and D is the contact between the breccia and the basement, whereas the dashed white line represents the boundary between the quartzite basement and an amphibolite dike also forming part of the basement. The orange and yellow stars in B, C, and D are located at the same point for reference between these subfigures.

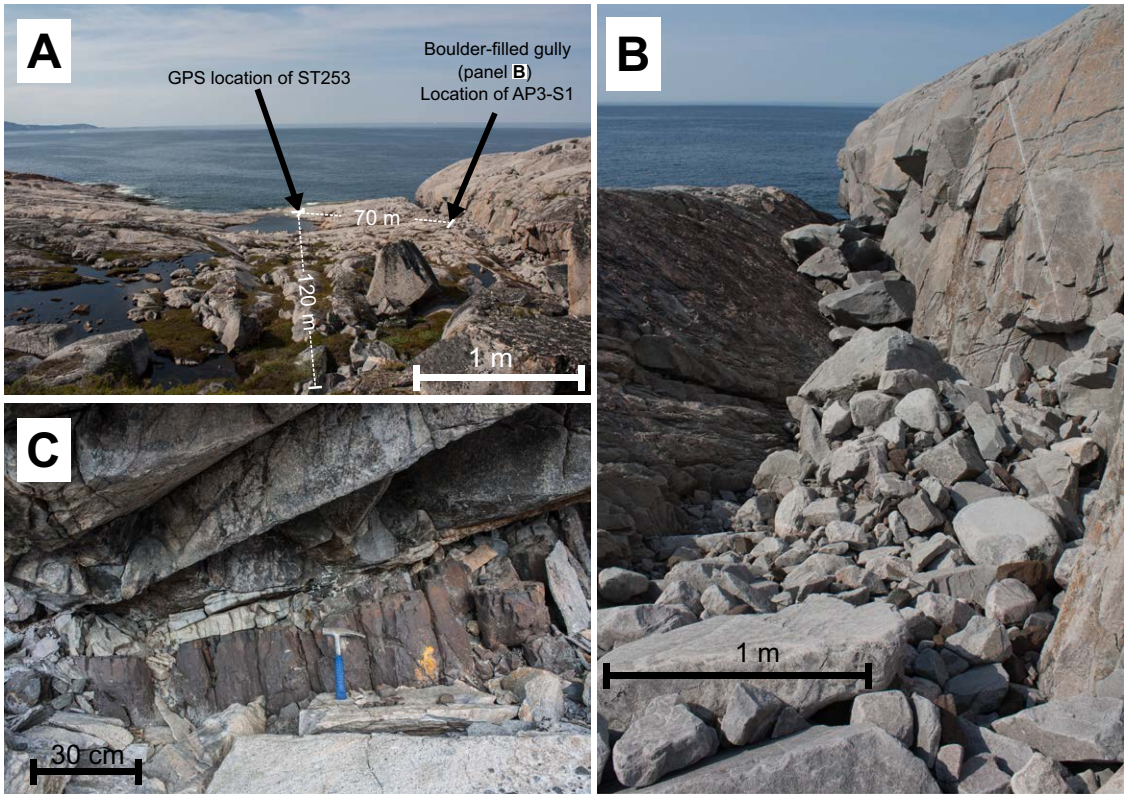

Figure 6. (A) An overview looking north of the area surrounding the global positioning system (GPS) location of ST253 in Tappe et al. (2007) taken from the location of the in situ dike shown in C. (B) Looking north onto out of situ boulders in the gully 70 m away from ST253. Two rock types of boulders were present in this gully: (1) granite and (2) olivine clinopyroxenite. Our sample AP3-S1 is olivine clinopyroxenite. (C) A relatively good exposure of in situ dike 120 m away on a bearing of 170° from AP2-ST253, which may have been part of the dike contributing to the boulders in the gully.

Figure 7. Looking northwest from the location of sample ST254. A good exposure of the Cape Strawberry Granite was observed at ST254, but no nephelinite dikes were observed at this location. This is the location of the only sample $^{40}Ar/^{39}Ar$ dated by Tappe et al. (2007), to which the rest of the Early Cretaceous nephelinite suite is tied.

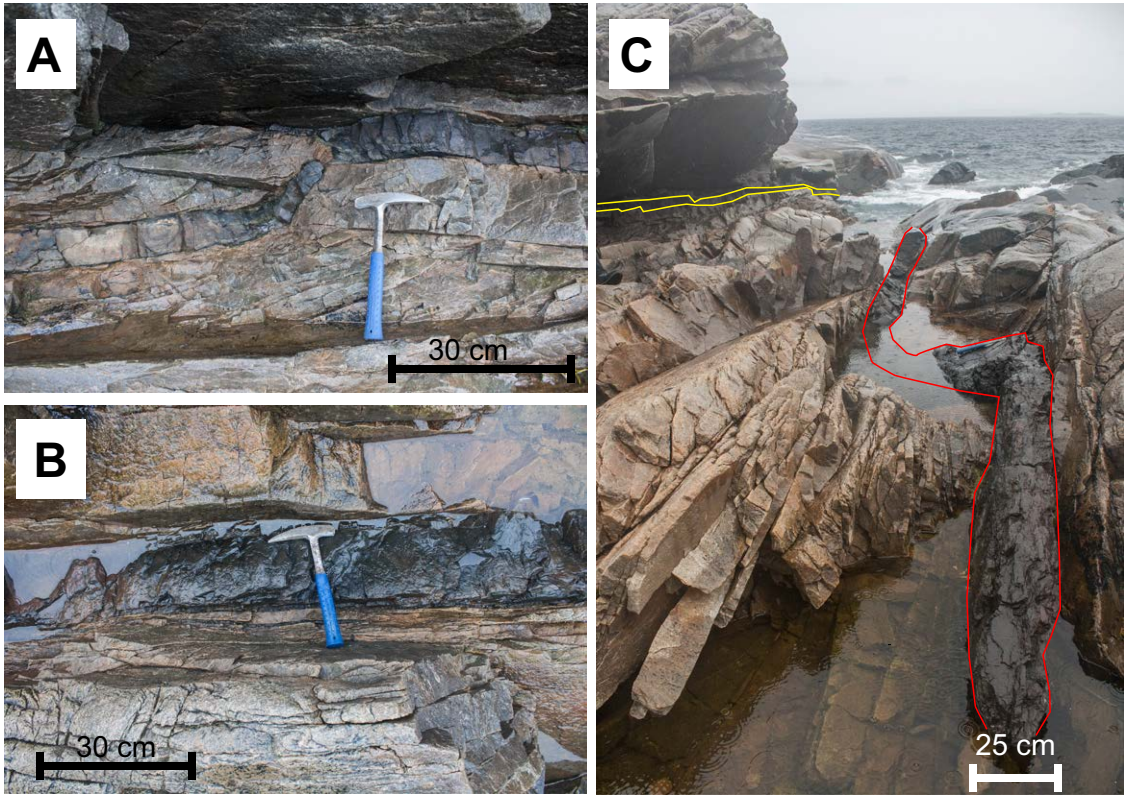

Figure 8. (A) Looking north toward a bridge structure in a small dike (sample AP4-S1) observed 15 m south of the global positioning system location of ST245. (B) 17 m away from ST245 looking down (north up) onto the other dike observed at this location (sample AP4-S2). (C) Looking east onto location AP4 depicting dikes from which samples AP4-S1 (yellow outline) and AP4-S2 (red outline) were obtained. The dike from which sample AP4-S2 was obtained also contains a bridge structure.

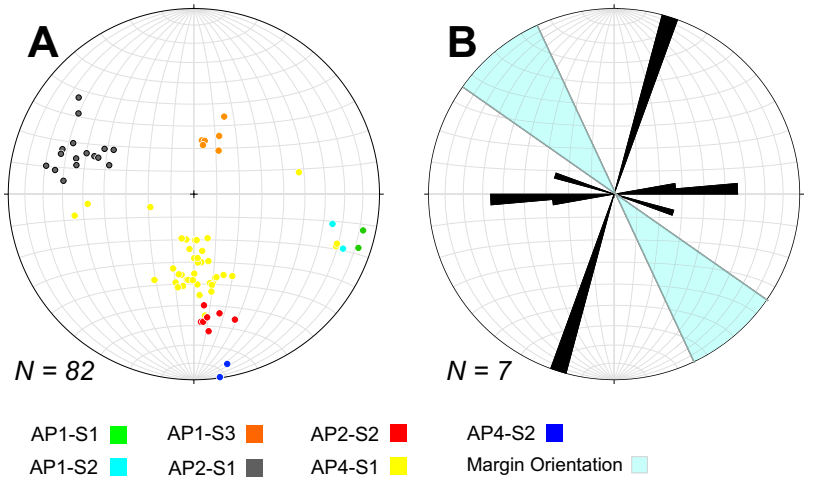

Figure 9. (A) Stereonet of poles to planes for the dike contacts at the sample localities. (B) Rose diagram using 5° bins of the dike contacts using the mean value of each dike contact data set plotted alongside the margin orientation (130° and 150°) derived using the modern coastline on satellite imagery.

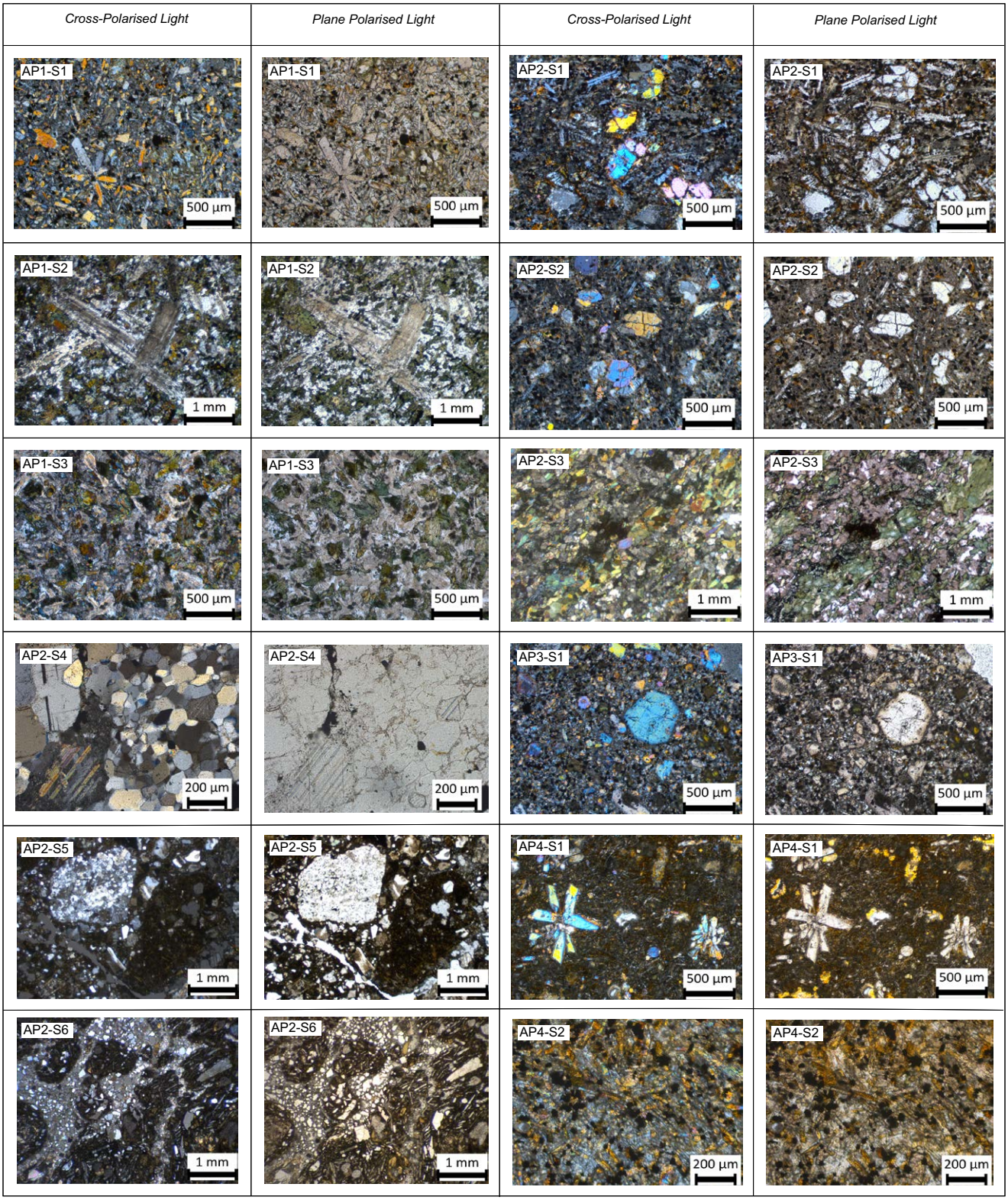

Figure 10. Thin section micrographs in both plane and cross-polarized light for all the samples described herein.

There is no observable metamorphic mineral fabric in AP1-S1. The SiO_2 content of sample AP1-S1 is too low to use the total alkalies versus silica (TAS) classification (Le Bas et al., 1986), but it can be classified as a lamprophyre (Woolley et al., 1996; Rock, 1986) due to the mineral assemblage and composition. Lamprophyre dikes are well studied and known to be extensive in the area (Foley, 1989).

Sample AP1-S2 was collected from a dark green dike. The most abundant mineral phase is chlorite (50%), which occurs as clusters of multiple crystals in the groundmass. This sample also contains altered plagioclase (30%), amphibole (10%), and apatite (<2%). No metamorphic mineral fabric was observed in sample AP1-S2. Sample AP1-S2 was classified as a basanite according to the TAS classification (Le Bas et al., 1986).

The dike from which sample AP1-S3 was obtained has a red-brown weathered surface and a blue-gray clean surface. The most abundant mineral phase in AP1-S3 is plagioclase (60%) occurring as highly altered interlocking crystals. Chlorite (25%) is the next most abundant mineral phase and occurs as both individual crystals and clusters. Other minerals present with abundances <5% in sample AP1-S3 include: amphibole, titanite, apatite, and pyrite. As with the other two samples collected at AP1, no mineral fabric is present in AP1-S3. Sample AP1-S3 was classified as a basaltic trachyandesite according to the TAS classification (Le Bas et al., 1986).

In addition to the different mineral assemblages, all the samples analyzed from the AP1 location have notably different compositions according to the XRF data (Table 4) with the alkali ($Na_2O + K_2O$) content of the AP1 samples not being as variable as the SiO_2 content (Fig. 11). The XRF data from the Makkovik Peninsula shows that SiO_2 content is lowest in AP1-S1 and highest in AP1-S3, which is the most felsic of all the samples analyzed. The sample with the composition most similar to the data collected by Tappe et al. (2007) is AP1-S1. In summary, the AP1 samples (AP1-S1, AP1-S2, and AP1-S3) have been classified as olivine lamprophyre, basanite, and basaltic trachyandesite, respectively. Of particular note, however, was the absence of the mineral phase nepheline in all the samples collected at this location.

Ford's Bight

Samples AP2-S1 and AP2-S2 were obtained from two separate dikes but are virtually indistinguishable from one another in thin section (Fig. 10), both texturally and mineralogically. The main mineral phases in both AP2-S1 and AP2-S2 are melilitite (70%) and olivine (20%), resulting in our classification of these dikes as olivine melilitite according to the classification of Woolley et al. (1996). Olivine melilitite is the expected composition at this location according to previous work by Tappe et al. (2007). No metamorphic mineral fabric was observed in either AP2-S1 or AP2-S2.

The XRF major element analysis of AP2-S1 and AP2-S2 demonstrates that these samples have very similar compositions (Fig. 11; Table 4). There are, however, several small, but notable compositional differences between these two dikes in that sample AP2-S1 has slightly higher SiO_2 and total alkali values than sample AP2-S2 (Fig. 11). Comparison of the major element XRF data obtained from our AP2 dike samples (AP2-S1 and AP2-S2) with the major element composition of sample ST103 (Fig. 11) obtained by Tappe et al. (2007) demonstrates that all three of these samples have very similar compositions and may represent samples collected from the same dike.

The two types of metamorphosed basement observed at the AP2 sample sites are an amphibolite (sample AP2-S3) and quartzite (sample AP2-S4) (Figs. 5B, 5C). Sample AP2-S3 contains amphibole (45%), highly altered plagioclase (35%), epidote (10%), and chlorite (10%). Sample AP2-S4 contains quartz (80%),

TABLE 4. X-RAY FLUORESCENCE DATA

	AP1-S1	AP1-S2	AP1-S3	AP2-S1	AP2-S2	AP3-S1	AP4-S1	AP4-S2
SiO_2	38.93	44.96	53.66	34.43	32.17	39.19	42.62	43.98
TiO_2	2.63	3.31	0.74	2.10	2.15	2.44	1.92	1.90
Al_2O_3	12.93	13.42	17.15	10.79	10.18	12.34	14.33	14.68
Fe_2O_3	13.77	16.91	9.45	11.43	12.04	12.43	12.03	11.87
MnO	0.23	0.33	0.21	0.23	0.24	0.21	0.21	0.18
MgO	8.09	5.36	4.85	10.66	10.96	9.07	6.93	8.45
CaO	11.25	6.94	5.97	16.00	14.52	13.55	10.19	9.99
Na_2O	2.78	3.25	3.14	2.00	2.22	2.26	2.67	2.93
K_2O	1.91	1.00	2.39	2.57	1.99	1.73	1.54	1.75
P_2O_5	1.02	1.86	0.18	2.31	2.58	0.86	0.65	0.66
SO_3	0.33	0.01	<0.002	0.82	1.04	0.20	0.15	0.16
CrO_3	0.02	0.00	<0.001	0.02	0.02	0.04	0.03	0.03
NiO	0.01	0.00	0.00	0.02	0.02	0.02	0.02	0.02
LOI	5.61	2.27	1.88	5.29	8.40	5.18	6.15	2.73
Total	99.51	99.63	99.62	98.67	98.52	99.51	99.44	99.34

Note: The results of X-ray fluorescence analyses for major element oxides in the dike samples (AP prefix) collected during this study. LOI—loss on ignition.

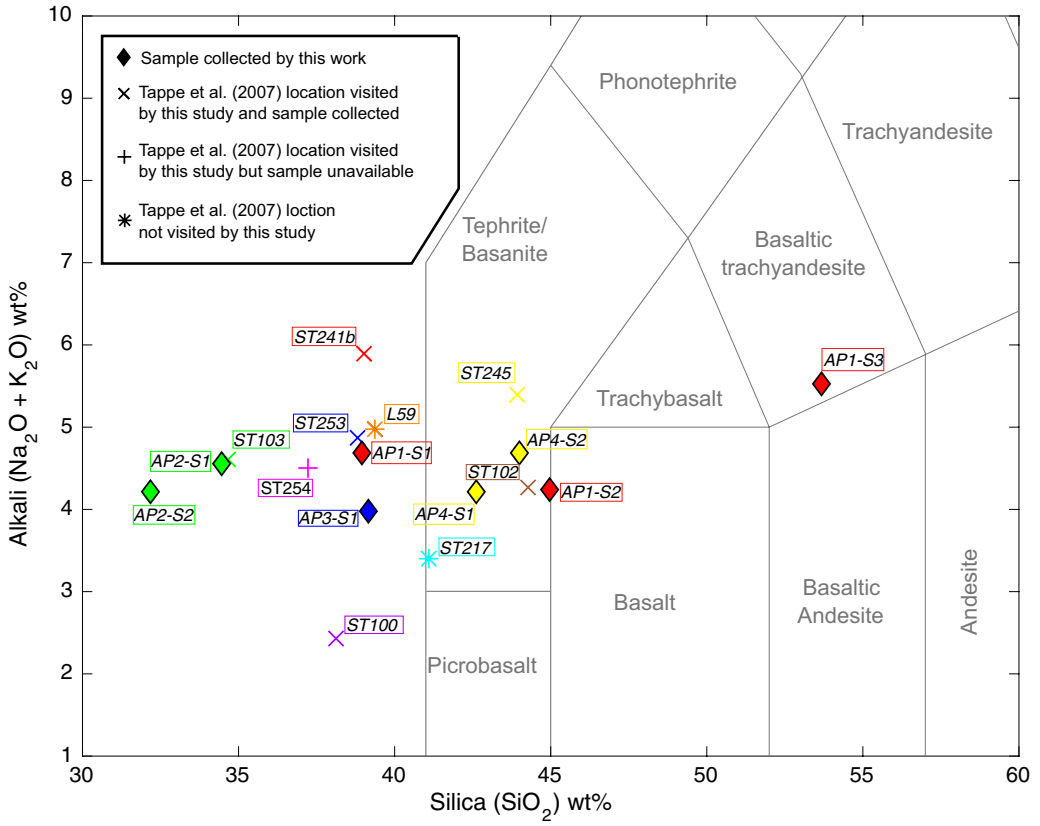

Figure 11. Total alkalies versus silica plot (Le Bas et al., 1986) depicting the dike samples collected and analyzed by this study along with the Early Cretaceous nephelinite suite of Tappe et al. (2007). Samples of the same color represent the same location.

garnet (7%), calcite (7%), plagioclase (4%), and opaque minerals (2%). Both samples AP2-S3 and AP2-S4 display a distinct metamorphic mineral fabric (Supplemental Materials 1; see footnote 1). The exposure of these lithologies is limited to a few square meters. However, both dikes (samples AP2-S1 and AP2-S2) were observed to continue into these metamorphosed units (Figs. 5B, 5C). The extent of the continuation of the younger dikes into the metamorphic basement could not be quantified due to lack of exposure.

The final lithology present at the AP2 sample site is a diatreme breccia that hosts the two dikes (samples AP2-S1 and AP2-S2). The diatreme breccia was observed as two distinct varieties, as characterized in samples AP2-S5 and AP2-S6. Sample AP2-S5 was taken from the breccia located at AP2 (Figs. 5C, 5D) but is also representative of the nearby boulders on the beach (Figs. 5A, 5E), whereas sample AP2-S6 was taken from a large boulder 45 m away from the rest of the AP2 samples on a bearing of 025° (Fig. 5E). AP2-S5 is green in outcrop, whereas AP2-S6 is dark yellow. This color variation is a reflection of AP2-S5 having a higher ratio of clasts to matrix compared to AP2-S6. The clast types found in both the breccia samples are very similar, mostly consisting of highly variable amounts of quartzite basement, amphibolite dike, olivine melilitite dike, and fragments of individual crystals primarily including but not limited to quartz, olivine, microcline feldspar, and plagioclase. Most clasts are angular, except the melilitite inclusions, which are typically rounded with an undulose texture at their perimeters. Clast size in both AP2-S5 and AP2-S6 is extremely variable, ranging from <0.1 mm to >10 cm. The matrix in both the AP2-S5 and AP2-S6 samples is predominantly carbonate.

Cape Strawberry

The eastern tip of Cape Strawberry (AP3, Fig. 3) is an area of exceptionally well exposed basement rocks (Fig. 6A) that were not observed to be intruded by dikes of any type. However, a distinct gully (Fig. 6B) filled with two types of boulders (granite and a mafic igneous material) was noted. The mafic igneous

material in this gully provided sample AP3-S1. The boulder from which AP3-S1 was obtained has a red-brown weathered surface and a dark gray clean surface. In hand specimen, calcite-infilled vesicles (to 7 mm) and olivine phenocrysts are visible. The dominant mineral phases in this sample are olivine, both fresh (20%) and serpentinized (15%), along with clinopyroxene in the groundmass (25%) and as a larger crystal phase (15%). The SiO_2 content of sample AP1-S1 is too low to use the TAS classification (Le Bas et al., 1986), but it can be classified as a lamprophyre (Woolley et al., 1996; Rock, 1986) due to the mineral assemblage and composition.

The XRF major element analysis of AP3-S1 (Fig. 11; Table 4) demonstrates that it is compositionally very similar to the igneous rocks sampled by Tappe et al. (2007) near this location, having a nearly identical SiO_2 value but slightly lower alkali content. However, given that AP3-S1 does not contain the mineral phase nepheline, as expected the dike from which AP3-S1 was collected does not belong to the nephelinite suite. The nearest in situ outcrop of the olivine lamprophyre composing the boulders in the gully was 120 m away from the location of ST253 (Fig. 6C).

North of Ikey's Point

In outcrop the weathered surface of the dike from which sample AP4-S1 was obtained varies from dark gray through to reddish-brown. The dominant mineral phase in sample AP4-S1 is clinopyroxene, occurring in both the groundmass (40%) and as larger crystals (20%). Olivine also occurs in AP4-S1 as a serpentinized (10%) and unaltered variety (5%). Vesicles with a calcite infill are common in AP4-S1. The XRF data obtained from AP4-S1 (Fig. 11; Table 4) indicate that this sample is a basanite according to the TAS classification of Le Bas et al. (1986).

Sample AP4-S2 was obtained from a separate dike 5 m south of the dike from which sample AP4-S1 was collected (Fig. 8). This second dike is slightly wider, 25 cm; in outcrop it is brown and more fractured and weathered than the previous dike. Sample AP4-S2 contains clinopyroxene (50%), plagioclase (20%), and olivine. Some minor opaque minerals are also present in AP4-S2 along with numerous calcite-infilled vesicles. AP4-S2 was classified as a basanite based on the major element composition derived using XRF and plotted on a TAS diagram (Fig. 11).

Although both AP4-S1 and AP4-S2 were classified as basanites, slight compositional differences between the two samples are apparent in the XRF major element data (Fig. 11; Table 4). These results show that AP4-S2 has a slightly higher SiO_2 and alkali content than AP4-S1. Given this slight compositional variation between these two dikes, it is very likely that these two dikes represent the same magmatic event, particularly given the similar orientations (Fig. 9). Overall our observations and analysis of the data collected at the AP4 location in the area north of Ikey's Point indicate that Early Cretaceous magmatism north of Ikey's Point may comprise two small (13 and 25 cm wide) basanite dikes.

BATHYMETRY, SEDIMENT THICKNESS, AND CRUSTAL STRUCTURE

An analysis of the degree of symmetry displayed in the bathymetry, sediment thickness, and crustal structure of the conjugate margins of the Labrador Sea is presented here to complement the asymmetry shown in the magmatic distribution in the preceding discussion (Fig. 12). To assess the margin symmetry displayed in the NOAA total sediment thickness (Whittaker et al., 2013) data and the global bathymetry data set (Smith and Sandwell, 1997), profiles approximating the traces of seismic lines BGR77–17, BGR77–21, and BGR77–12 (Fig. 1A) were created (Fig. 12). These profiles were then extended along the same trajectory as their corresponding seismic line until they reached the modern coastline, thus allowing us to study the full width of the continental shelf. Our observations of conjugate margin asymmetry are summarized in Table 5.

Figure 12A displays the Smith and Sandwell (1997) global bathymetry data set for the Labrador Sea. The Labrador Sea has a maximum depth of ~3500 m, with water depths mostly <200 m on both continental shelves (Fig. 12B). The continental shelf is ~150 km wide offshore Labrador compared to southwest Greenland, where it is mostly <50 km wide. The profiles (Fig. 12B) show that the continental shelf remains relatively consistent in width along the southwest Greenland margin, whereas on the Labrador margin it increases to the north.

The distribution of sediments between the margins of the Labrador Sea is highly asymmetric (Welford and Hall, 2013). The Labrador margin displays considerably thicker and more extensive synrift and postrift sedimentary sequences compared to the southwest Greenland margin (Figs. 12C, 12D, and 13). The Labrador margin is dominated by a large margin-parallel basin containing in excess of ~8000 m of sediments for much of its length (Fig. 12C). This basin is particularly prominent in the central and northern segments of the margin, where isolated areas contain more than ~11,000 m of sediment infill. Even outside this main basin it can be seen that for a large region extending from ~50 km to ~300 km offshore, a more diffuse area containing ~3000–6000 m of sediment infill is present. This region is much wider at the northern end of the margin compared to the south. In contrast, sediment infill on the southwest Greenland margin is significantly thinner and less spatially extensive than its Labrador conjugate. On the southwest Greenland margin sedimentary basins with thicknesses in excess of 4000 m are absent, with most areas containing <2000 m of sedimentary infill. Thus, comparison of sediment thickness along profiles 1, 2, and 3 (Fig. 12D) supports the observation of significantly more sediment deposition on the Labrador margin consistently along the length of the margin. It is interesting that the distance between the start of the profile (modern coastline) and the point of greatest sedimentary thickness appears to decrease from profile 1 in the south to profile 3 in the north. Profiles 1–3 in Figure 12D also demonstrate the differing basin geometry between these conjugate margins. On the Labrador margin the main margin-parallel basin appears to represent a distinct feature compared to the southwest Greenland

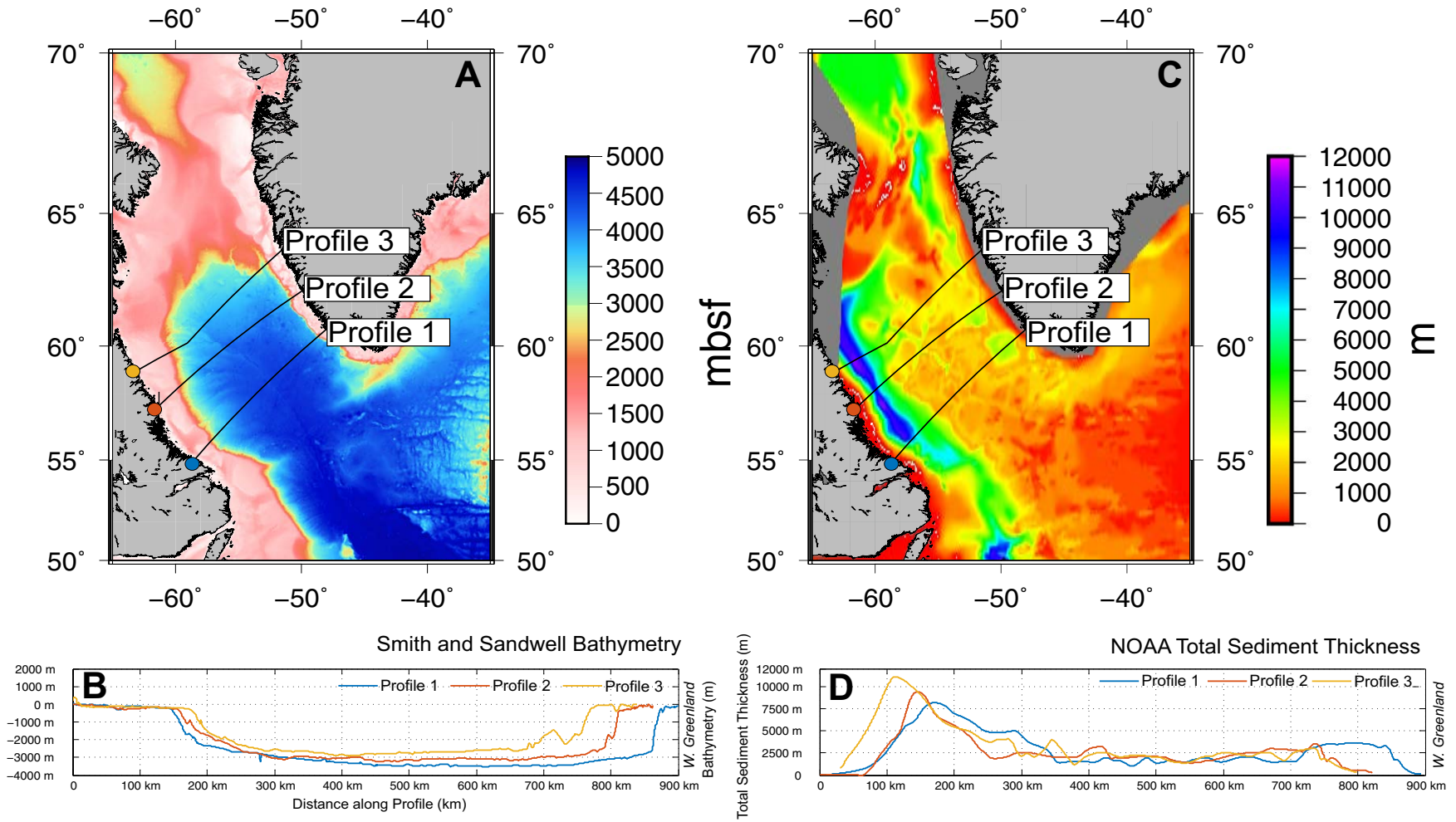

Figure 12. (A) Bathymetry of the Labrador Sea from Smith and Sandwell (1997) data; mbsf—meters below seafloor. (B) Bathymetric transects along profiles 1, 2, and 3. (C) Total sedimentary thickness in the Labrador Sea from the National Oceanic and Atmospheric Administration world's oceans and marginal seas total sedimentary thickness (version 2; Whittaker et al., 2013). (D) Total sedimentary thickness transects along profiles 1, 2, and 3. For C and D, the Labrador end of the transect is at the left (0 km) and the West Greenland end is on the right. Profiles 1, 2, and 3 approximately correspond to the seismic reflection lines BGR77–17, BGR77–21, and BGR77–12, respectively. The profiles used in this study have been extended along the same trajectory as their corresponding seismic line to the present coastline, thus allowing us to study the full width of the continental shelf.

margin where the sedimentary basins, if present, appear to have a less well defined, more diffuse appearance.

The crustal velocity model depicted in Chian et al. (1995b) that incorporates the data from Chian and Louden (1994) was used to assess asymmetry displayed in the crustal structure between the Labrador and southwest Greenland margins (Fig. 14). Previously workers (Keen et al., 1994; Chian and Louden, 1994; Chian et al., 1995a) considered the velocity structure of both the southwest Greenland and Labrador margins to be divided into three distinct zones (Fig. 14).

Zone 1 is characterized as a region that has a typical continental crustal velocity structure. On the Labrador margin zone 1 is ~140 km wide and is characterized by highly extended continental crust that has undergone consider-

TABLE 5. MAJOR STRUCTURAL AND MAGMATIC COMPONENTS OF THE LABRADOR AND SOUTHWEST GREENLAND MARGINS

	Labrador	Southwest Greenland
Continental shelf width (Figs. 4A, 4B)	Wide (~150 km)	Narrow (~50 km)
Maximum offshore sedimentary cover (synrift and postrift) (Figs. 12C, 12D, and Fig. 13)	~12,000 m	~3700 m
Onshore intrusive magmatism	Minor nephelinite suite proposed by Tappe et al. (2007) but disputed in this study	Summarized in Table 2
Offshore magmatism	Alexis formation and other volcanics in offshore wells (Table 3)	Unknown due to absence of offshore wells
Crustal-scale detachment faults	Possibly; inferred by the presence of distinct basin (Welford and Hall, 2013)	No

able subsidence. However, on the southwest Greenland margin zone 1 is only ~70 km wide and has undergone considerably less subsidence (Chian, et al., 1995a). Zone 2 represents a region of transitional crust located oceanward of zone 1 on both margins (Chian et al., 1995a). Compared to zone 1, zone 2 displays similar velocity characteristics, and is ~70–80 km wide on both margins. Zone 2 is characterized by a 5-km-thick region with a high velocity (6.4–7.7 km/s) overlain by a thin (<2 km) low-velocity region (4–5 km km/s). Zone 3 is characterized by typical oceanic crustal velocities and is oceanward of zone 2 on both margins.

DISCUSSION

Comparison of the Composition of the Makkovik Magmatism with Other Rift-Related Magmatism

The XRF results obtained during this study have been compared to other selected occurrences of rift-related magmatism globally (Fig. 15). The Yarmony Mountain lavas of the Rio Grande Rift (Leat et al., 1990) were selected for comparison because they are interpreted to represent small-volume, early rift-

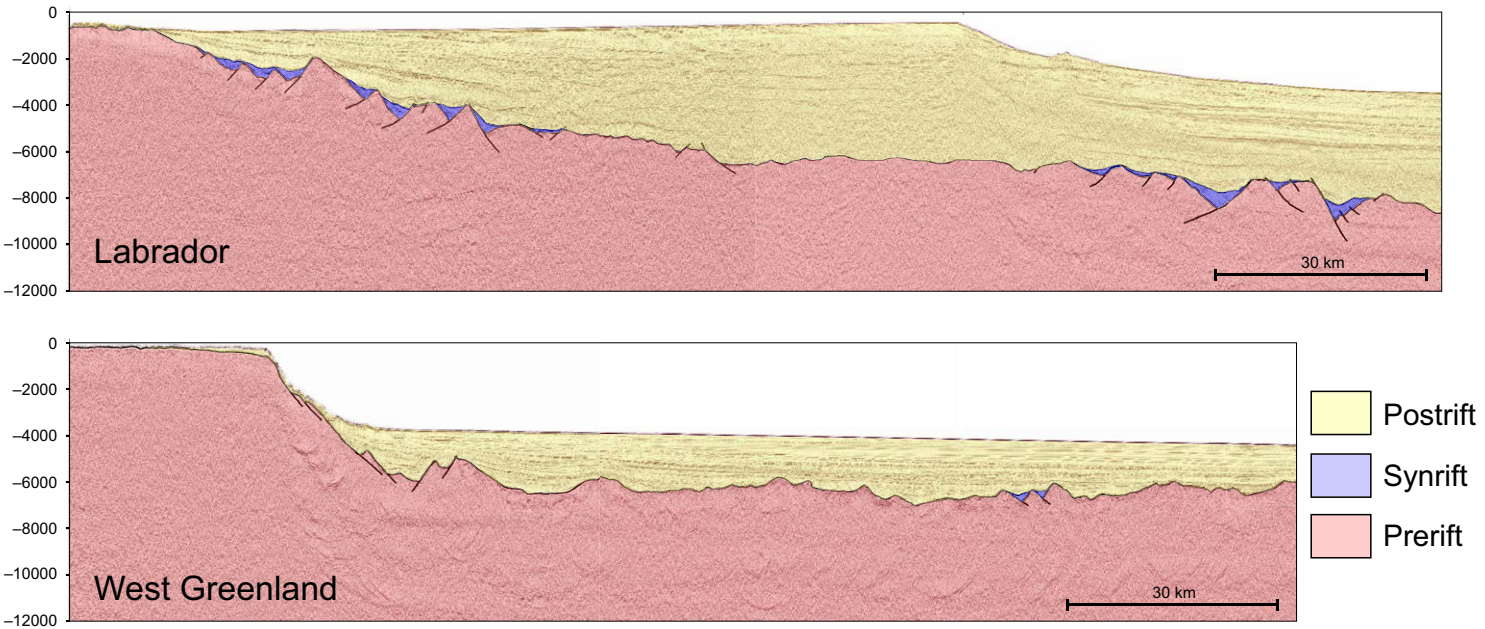

Figure 13. Segments of the two-dimensional seismic reflection profiles 90-3 and 90-1 (Keen et al., 1994) for the Labrador and southwest Greenland margins, respectively, with interpretations of the base postrift and base synrift. The location of these segments is depicted in Figure 1.

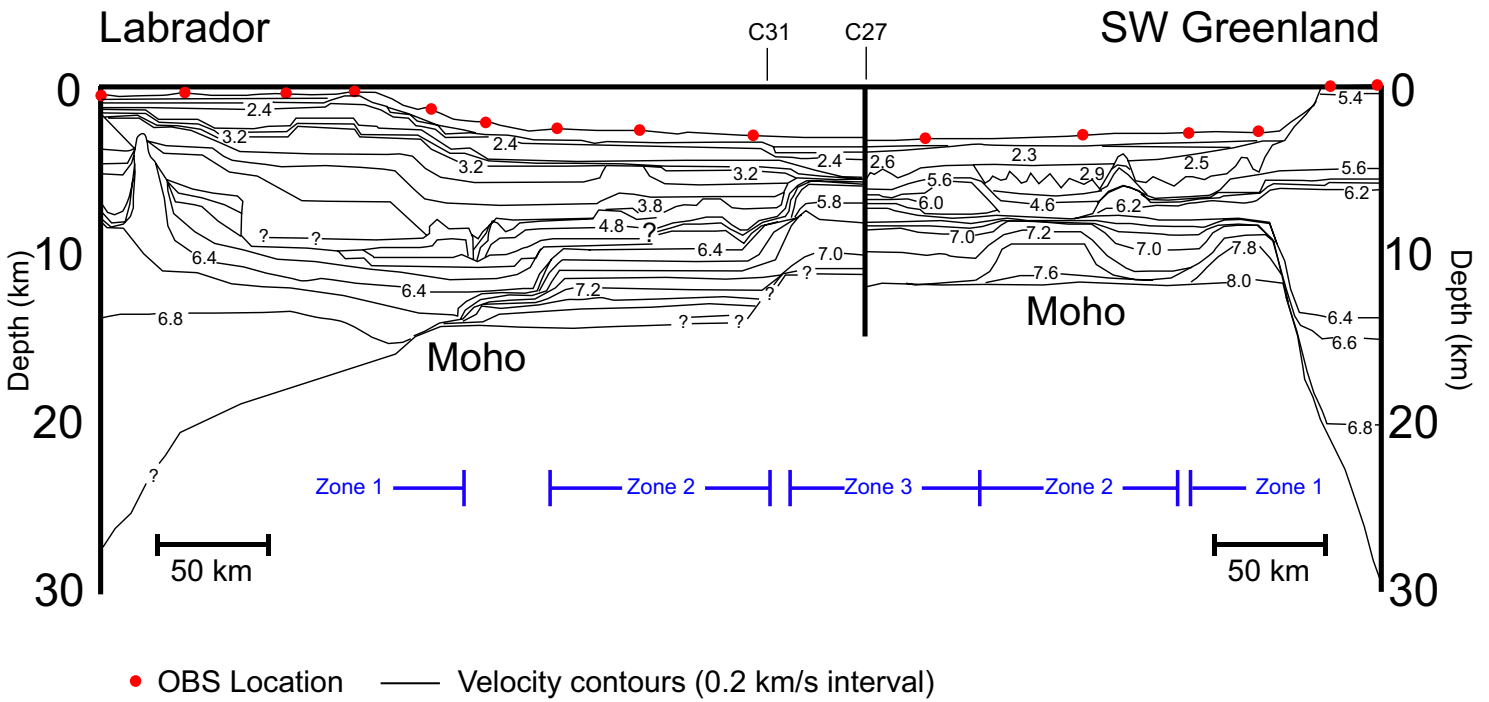

Figure 14. Velocity structure of the margins of the Labrador Sea reconstructed to polarity chron C27 (Danian) reproduced from Chian et al. (1995b). OBS—ocean bottom seismograph.

related melts, and therefore may have been produced in a geological setting similar to that of the proposed Early Cretaceous magmatism near Makkovik (Tappe et al., 2007). The Suez Rift magmatism (Shallaly et al., 2013) was selected because it contains a wide array of rift-related manifestations of magmatism, including sills, dikes, and extrusives. Two magmatic suites attributed to the Central Atlantic Magmatic Province (CAMP) are also included for comparison: Algarve in southern Portugal (Martins et al., 2008) along with the magmatism in Guyana and Guinea (Deckart et al., 2005). The CAMP magmatism was selected because it enables comparison with a widespread rift-related magmatic event that resulted in continental breakup.

Comparing the composition of the Makkovik Early Cretaceous nephelinite suite (Tappe et al., 2007) with other selected occurrences of rift-related magmatism shows that it is compositionally more diverse than any of the other magmatic suites considered (Fig. 15), displaying greater variation in both the alkali and silica values than any of these systems. Although it is extremely unlikely that all of the AP samples belong to the Early Cretaceous nephelinite suite (particularly sample AP1-S3), the more mafic AP samples depict a similar range of silica values to the Early Cretaceous nephelinite suite. The Tappe et al. (2007) samples show considerably higher variation in total alkali values than the AP samples or any of the other data sets included for comparison. The wide range of compositions found in the Early Cretaceous nephelinite suite (Tappe et al., 2007) may imply that not all of the dikes analyzed by the previous work are part of the same event.

Extent of Mesozoic Magmatism around Makkovik

Given the relatively close proximity of Makkovik to observations of Early Cretaceous magmatism in offshore wells (Fig. 1; Table 3), it would not be unreasonable to observe evidence of contemporaneous early rift-related magmatism cropping out onshore. Our field observations, however, indicate that the Early Cretaceous magmatism around Makkovik is volumetrically and spatially extremely minor compared to the numerous stages of extensive, readily observable intrusive magmatism that preceded it (e.g., Foley, 1989) and the well-documented magmatism on the conjugate southwest Greenland margin (Larsen et al., 2009). Although the field study area around Makkovik (Fig. 3) is significantly smaller than the extent of the dikes observed in southwest Greenland, no other evidence for Mesozoic magmatism has been recorded elsewhere onshore Labrador.

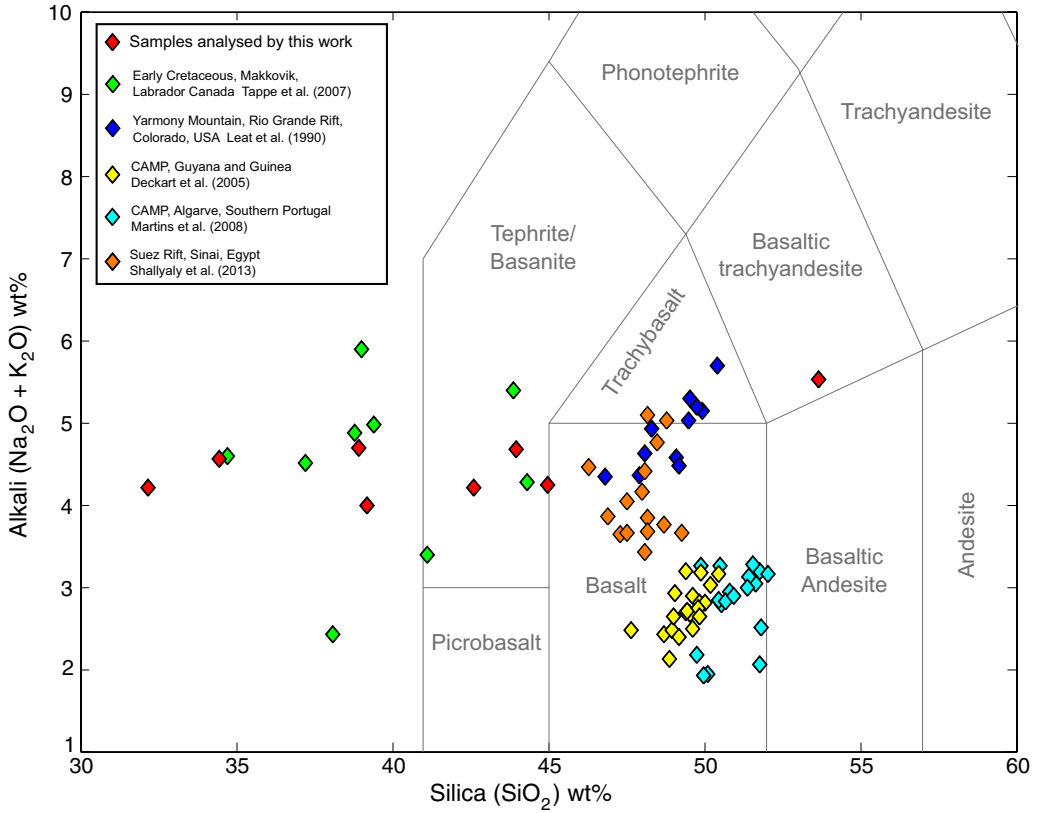

Figure 15. Total alkalies versus silica plot (Le Bas et al., 1986) depicting the dike samples collected and analyzed by this study along with the Early Cretaceous magmatic suite near Makkovik (Tappe et al., 2007), the Rio Grande Rift, Yarmony Mountain lavas (Leat et al., 1990), the Suez Rift (Shallaly et al., 2013), and the Central Atlantic Magmatic Province (CAMP) in Algarve, southern Portugal (Martins et al., 2008) along with Guyana and Guinea (Deckart et al., 2005).

Of the seven sample locations in Tappe et al. (2007) visited during this study none provided clear, undisputable evidence for belonging to a contiguous Early Cretaceous magmatic event. We think it is also exceptionally unlikely that the outcrops were removed by subsequent erosion between this study and the work of Tappe et al. (2007). Our observations on the peninsula north of the town of Makkovik (AP1) and on Cape Strawberry (AP3) did not provide sufficient evidence for the Early Cretaceous magmatism previously described at these locations. The most reliable evidence confirmed by this study for the magmatism characterized by Tappe et al. (2007) as Early Cretaceous was found in Ford's Bight (AP2, Fig. 5) and north of Ikey's Point (AP4, Fig. 8).

Our AP2 sample location in Ford's Bight is in very close proximity to the diatreme originally described as a sedimentary breccia by King and McMillan (1975) and later as a diatreme by Wilton et al. (2002). Our field observations concur with that of Wilton et al. (2002) that the AP2 sample location is part of the previously documented Ford's Bight diatreme. This confirms that of the nine samples stated as belonging to the Mesozoic dike suite in Tappe et al. (2007) (Table 1), three are part of a diatreme, not a dike swarm as previously claimed, with two of the Ford's Bight samples locations not containing in situ outcrop. Within the diatreme there are dikes present, but it is misleading to imply that they are part of a singular geographically widespread intrusive event that can be described as the nephelinite suite. The diatreme was mentioned in Tappe et al. (2007, p. 438) as "poorly described mafic dikes cutting a breccia bed"; however, it is not made clear that this area is either (1) the location of three of their samples or (2) a diatreme rather than a dike swarm. Furthermore, confirming that ST103 is, as expected, an olivine melilitite demonstrates that there is unlikely to be a problem associated with the original acquisition or our use of the coordinates provided by Tappe et al. (2007) and the original characterization of the mineralogy at ST103. The geological context of the dikes needs clarifying, because the observed dikes in Ford's Bight are intrinsically associated with the diatreme (Wilton et al., 2002)

and do not appear to be associated with a regional-scale intrusive event such as that described in Tappe et al. (2007). However, if the biostratigraphic age provided by King and McMillan (1975) of 197–145 Ma is correct, then this is currently the most reliable evidence in the area for Mesozoic magmatism, with the fossils possibly being derived from the maar above the diatreme (White and Ross, 2011).

Our analysis also indicates that one of the dikes north of Ikey's Point at AP4 is likely to be that described and sampled by Tappe et al. (2007), the other basanite dike at this location being part of the same event. However, even if one or both of the dikes at AP4 is the dike analyzed by Tappe et al. (2007), they are extremely small (13 cm and 25 cm wide) and localized.

Comparison of the XRF data with other suites of rift-related magmatism globally has demonstrated that the nephelinite suite (Tappe et al., 2007) is compositionally much more diverse than the other events considered (Fig. 15). This observation provides further evidence that the samples collected by Tappe et al. (2007) might not form part of the same magmatic event.

Overall, our comparison of the field relationships, orientation, mineralogy, and composition of the samples collected at the locations of the samples prefixed with AP2 and AP4, where some evidence for the Early Cretaceous magmatism described by Tappe et al. (2007) was found, suggests that there is no reason to attribute the exceptionally different style of magmatism in Ford's Bight (AP2) and north of Ikey's Point (AP4) to the same event.

Furthermore, given that the one location in this dike suite that was dated by $^{40}Ar/^{39}Ar$ methods by Tappe et al. (2007) (sample ST254) was found to not contain any exposed comparable dikes, the coherence of the proposed Early Cretaceous nephelinite suite as being as a result of a singular magmatic event should be reconsidered. In terms of the age of the nephelinite suite characterized by Tappe et al. (2007), the plateau age from the $^{40}Ar/^{39}Ar$ dating is not defined by a continuous outgassing plateau and the two segments used in each are considerably less than the 50% gas release generally accepted as the hallmark of a reliable step-heating age. Even when the two segments in Tappe et al. (2007) are combined, it seems that the total gas fraction plateau used is only 52%, i.e., only just above 50%. In addition, another problem with the $^{40}Ar/^{39}Ar$ date of Tappe et al. (2007) is the fact that the inverse isochron age is well outside of error and the plateau age is far from the atmospheric value. Thus the $^{40}Ar/^{39}Ar$ age of 142 Ma for sample ST254 is of marginal reliability.

Another aspect of the Early Cretaceous magmatism on the Labrador margin that remains unclear is why the orientations of the dikes observed by Tappe et al. (2007) are described as predominantly east-west. If these dikes are rift related, then they would be expected to have been intruded under the influence of the extensional stress field parallel to the rift axis i.e., coast parallel as they are in southwest Greenland (Larsen et al., 2009). Although the only compositionally appropriate east-west dikes observed by this study were at Ikey's Point (AP4), should a larger suite exist with this orientation it would not be compatible with simple northeast-southwest–trending Mesozoic rifting, culminating in the opening of the Labrador Sea (Abdelmalak et al., 2012).

Implications for Early Rifting of the Labrador Sea Region

The results of this study have demonstrated that considerable asymmetry exists in many aspects of the conjugate margins of the Labrador Sea, including the distribution of rift-related magmatic rocks, the bathymetric expression, the sediment distribution, and the crustal structure. These observations of asymmetry may support a simple shear mode of rifting (Fig. 16). Here we systematically evaluate our observations of asymmetry against the predictions of the Lister et al. (1986) simple shear model of passive margin formation that has been previously applied to explain the observed asymmetry in many conjugate margin pairs and rift systems including the Greenland-Norway conjugate margins (Torske and Prestvik, 1991) and the south Atlantic (Becker et al., 2016). Of particular importance when evaluating the simple shear model (Lister et al., 1986) is whether the polarity of the different aspects of asymmetry all agree with the predictions of the model.

A full comparison of the extent of rift-related magmatism on the margins of the Labrador Sea is inhibited by the absence of well data offshore southwest Greenland (Fig. 1A). The nearest offshore well on the Greenland side of the Labrador Sea is Qulleq-1, which is much farther north in the Davis Strait (Fig. 1A), and is influenced more by transform margin tectonics rather than the rifted margin regime in the Labrador Sea (Wilson et al., 2006).

Although the absence of well data offshore southwest Greenland prevents us from making a full comparison of the volume of rift-related magmatism, this study has shown that the Early Cretaceous magmatism identified onshore in Labrador by Tappe et al. (2007) is considerably less extensive than that observed on the coast parallel dikes onshore in southwest Greenland (Larsen et al., 2009). This allows us to state that there is an asymmetric distribution in the extent of the exposed onshore Mesozoic magmatism between the Labrador margin and the southwest Greenland margin. This asymmetric distribution of rift-related magmatism supports the predictions of the simple shear model of passive margin formation, whereby the center of the melt generation may have been offset from the central rift axis (Fig. 16A), resulting in a greater amount of melt on the upper plate southwest Greenland margin (Fig. 16A). That is, the greater extent of coast-parallel dikes in southwest Greenland suggests that the southwest Greenland margin may represent the upper plate margin in a simple shear system.

Magmatic underplating on the upper plate margin is another prediction of the Lister et al. (1986) simple shear model. High-velocity zones have been observed in seismic studies on these conjugate margins, but whether they represent serpentinized peridotite (Reid and Keen, 1990) or magmatic underplating (Keen et al., 1994) is debatable (Chian et al., 1995b). Chian et al. (1995b) determined that serpentinized peridotite is more consistent with the observations than magmatic underplating. Due to the inconclusive nature of these observations, we have chosen not to use them as evidence in our analysis of the applicability of the simple shear model (Lister et al., 1986) to the margins of the Labrador Sea. However, magmatic underplating might help to explain the absence of significant postrift sedimentary basins offshore southwest Green-

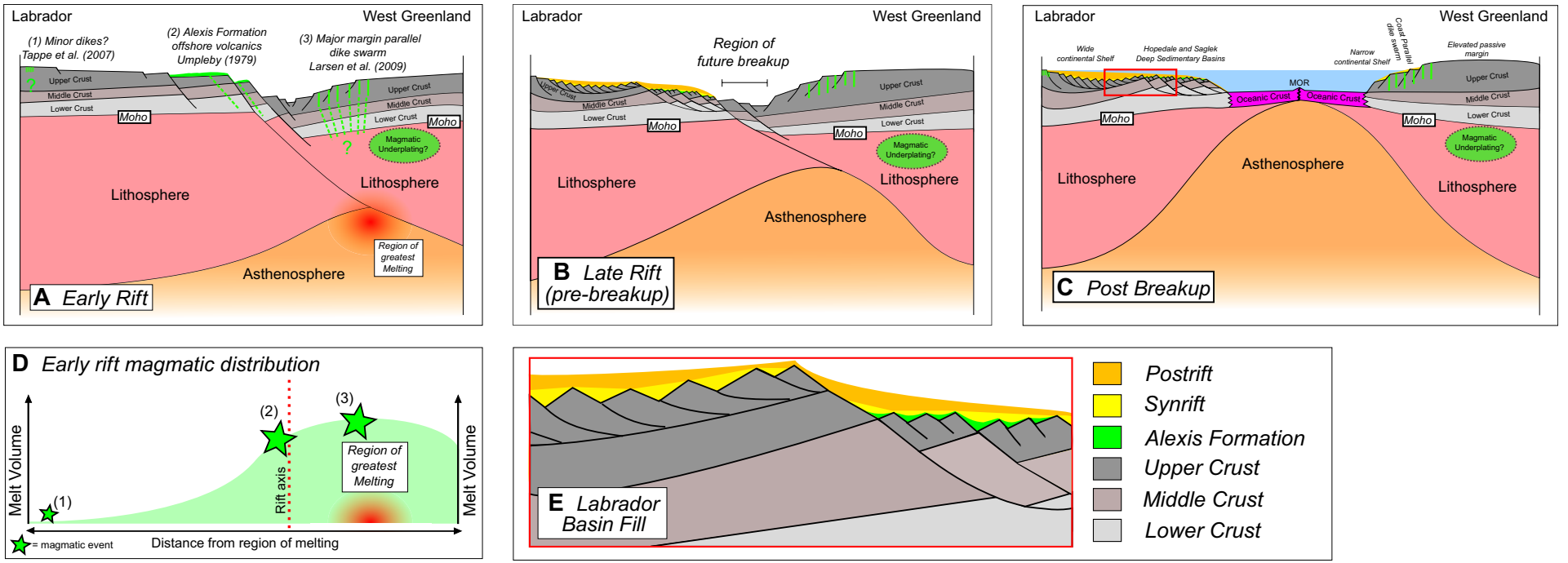

Figure 16. (A) Conceptual model of early continental rifting prior to the opening of the Labrador Sea under a simple shear rifting regime. (B) Conceptual model of late continental rifting. (C) Schematic depiction of the post-breakup (present) architecture of the conjugate passive margins of the Labrador Sea showing the preserved architecture from the early simple shear rifting modified from Lister et al. (1986), including the wide and narrow continental shelves for the Labrador and Greenland margins, respectively, the deep sedimentary basins offshore Labrador, and the minimal offshore sedimentary cover and elevated passive margin on the Greenland side of the rift. (D) The theoretical distribution of melt volumes against proximity to the rift axis where the region of melting is offset from the rift axis due to the simple shear–type early rifting. The three documented rift-related magmatic events included in green in A and D are (1) Early Cretaceous nephelinite dikes near Makkovik (Tappe et al., 2007); (2) the offshore Labrador volcanics (Umpleby, 1979); and (3) the coast-parallel dikes onshore southwest Greenland (Larsen et al., 2009). (E) Enlarged section off inset C in this figure showing the theoretical basin geometries on the upper plate Labrador margin.

land (Figs. 12C, 12D), as magmatic underplating could provide the additional buoyancy required to prevent significant postrift subsidence from occurring. Alternatively, the lack of postrift sedimentation offshore southwest Greenland could be due to a deficiency of sediment supply to the offshore basins; however, if this was the case we would still expect to observe deeper water depths.

Despite the obvious disparity in the extent of onshore rift-related intrusive magmatism between southwest Greenland and that near Makkovik, quantifying the melt volumes associated with rifting on each margin even approximately is problematic for a number of reasons. First, offshore magmatism cannot be accurately quantified on both margins given the sparse seismic and well data coverage. Second, it is difficult to estimate the contributions of magmatic underplating and other intrusives in the lower crust; these contributions were estimated by White (1992) to potentially represent three times the volumes of other intrusive and extrusive magmatic rocks on passive margins. However, it seems more likely that significant magmatic underplating is present in southwest Greenland due to the potential additional support this margin has received.

A wider continental shelf on the lower plate margin is another prediction of the simple shear model of passive margin formation (Lister et al., 1986). The asymmetric nature of the bathymetric profiles across the Labrador Sea depicted in this study (Figs. 12A, 12B) using the Smith and Sandwell (1997) bathymetric data is consistent with a model in which the Labrador margin would be the lower plate margin.

An asymmetric distribution of sedimentation as described in this study is also a prediction of the simple shear model of passive margin formation (Lister et al., 1986), the greater amount of sedimentary deposition occurring on the lower plate margin. The NOAA total sediment thickness data show that the Labrador margin has considerably deeper sedimentary basins (Figs. 12C, 12D), and thus would represent the lower plate margin in a simple shear system.

Another aspect of the sediment distribution on the margins of the Labrador Sea that supports the simple shear model is the geometry of the marginal basins. In the marginal basin on the Labrador margin the total sediment

thickness data profile depicts an abrupt increase in sediment thickness, as opposed to the southwest Greenland margin, where a much less apparent peak in sediment thickness is present. This abrupt increase in sediment thickness may imply a fault-controlled basin as opposed to the marginal basins offshore southwest Greenland, in which the NOAA data record more diffuse sedimentation.

The simple shear model implies a much greater degree of synrift structuring on the lower plate margin. Our analysis has demonstrated that the Labrador margin displays considerably greater synrift deformation and sedimentation than the southwest Greenland margin. The more significant synrift deformation and sedimentation on the Labrador margin supports a simple shear–dominated mode of early rifting with Labrador being the lower plate margin.

Welford and Hall (2013) calculated sediment difference (excess and deficiency), also using the NOAA sediment thickness data for the Labrador Sea. The work of Welford and Hall (2013) showed that most of the Labrador Sea appears from isostatic calculations to be deficient in sediments, whereas the Hopedale Basin is near balanced and the Saglek Basin has an excess of sediments. Welford and Hall (2007) showed that high gradients in the sediment excess and deficiency could indicate the presence of steep listric faults, a key component of a simple shear–dominated rifting regime, supporting a simple shear model of margin formation in the Labrador Sea.

The velocity structure of the margins of the Labrador Sea (Fig. 14; Chian et al., 1995b) also displays asymmetry consistent with a simple shear–dominated phase of early rifting. This is evident in zone 1 (stretched continental crust, Fig. 14), where this region is ~140 km wide on the Labrador margin compared to the southwest Greenland margin, where this zone occupies ~70 km. In the simple shear model of passive margin formation the greater amount of stretching, faulting, and subsequent subsidence occurs on the lower plate margin, which, as with the other observations made by this study, would be the Labrador margin. Using their velocity structure, Chian et al. (1995a) proposed a model of continental breakup whereby breakup occurred closer to the southwest Greenland margin. Breakup occurring closer to the southwest Greenland margin is consistent with the other observations implying that southwest Greenland may have constituted the upper plate margin.

Overall, the high degree of magmatic, sedimentary, and structural asymmetry observed between these two conjugate margins allows us to suggest a simple shear mechanism of early rifting, as opposed to rifting under a pure shear–dominated regime. Under a simple shear rifting regime the upper plate margin would be southwest Greenland and the lower plate margin would be Labrador, according to the distinction between the margin types in the original model by Lister et al. (1986). The asymmetry documented between these margins may have implications for petroleum exploration in the Labrador Sea (e.g., Jauer et al., 2014; Jauer and Budkewitsch, 2010). Such implications include the deeper, potentially more prospective basins on the Labrador margin and the inevitable asymmetry in the heat flow due to the asymmetric magmatic distribution, which may potentially influence the maturation of source material (Peace et al., 2015).

CONCLUSIONS

This study used the previous descriptions of Mesozoic rift-related magmatism (Tappe et al., 2007) to guide field work with the aim of understanding the controls on rifting in the region prior to the opening of the Labrador Sea. Through the field work and subsequent analysis of the data we have further characterized this event, demonstrating that certain aspects differ from the descriptions provided in the previous work. Our conclusions on the characteristics and extent of Early Cretaceous magmatism in proximity to the town of Makkovik are as follows.

1. Early Cretaceous magmatism around Makkovik, Labrador, is volumetrically and spatially extremely minor compared to the numerous other phases of extensive, readily observable intrusive magmatism exposed in the area.

2. Of the nine Early Cretaceous magmatism sample locations described by Tappe et al. (2007), we visited seven for this study. Only two of these seven localities provided any evidence for the magmatism described in the previous work.

3. Mesozoic magmatism is not sufficiently simple and consistent to consider this event as a single coherent intrusive suite of Early Cretaceous nephelinite dikes, as the outcrops are too sparse, variable, and unreliable. At least three of the Tappe et al. (2007) samples are actually from a diatreme, and the rest are either unobservable or ambiguous in nature.

4. The most reliable evidence for Mesozoic magmatism around Makkovik is the diatreme in Ford's Bight dated using fossil evidence by King and McMillan (1975). The diatreme was not observed to be part of a dike swarm as implied by the sample locations in Tappe et al. (2007).

Our conclusions on margin asymmetry, rifting mechanisms, and the relationship between Mesozoic magmatism in West Greenland and Labrador are the following.

1. The magmatic distribution across these two conjugate margins is extremely asymmetric, with the Mesozoic magmatism exposed at surface in the area around Makkovik being minor compared to observations of rift-related diking exposed at surface on the conjugate southwest Greenland margin.

2. This asymmetric magmatic distribution complements other observations of asymmetry, including deeper sedimentary basins and a wider continental shelf on the Labrador margin compared to southwest Greenland allowing us to propose a simple shear model for early rifting prior to the opening of the Labrador Sea, as opposed to a pure shear rifting model.

3. In a simple shear rifting model the southwest Greenland margin would be the upper plate margin and the Labrador margin would be the lower plate margin.

ACKNOWLEDGMENTS

Funding for this research was primarily provided by Royal Dutch Shell in the form of a CeREES (Centre for Research into Earth Energy Systems) studentship at Durham University. We thank the Durham University Center for Doctoral Training in Energy and the Durham Energy Institute for their contribution toward the costs of this research. This research would not have been possible

without the advice of Alana Hinchey of the Geological Survey of Newfoundland and Labrador; Henry Emeleus of the Department of Earth Sciences, Durham University; and the hospitality of the people of Makkovik. We also thank BGR (Bundesanstalt für Geowissenschaften und Rohstoffe, Hannover, Germany) and Schlumberger Limited for providing access to the seismic data and the Petrel seismic interpretation software, respectively. We acknowledge the contribution of the two anonymous reviewers.

REFERENCES CITED

Abdelmalak, M.M., Geoffroy, L., Angelier, J., Bonin, B., Callot, J.P., Gélard, J.P., and Aubourg, C., 2012, Stress fields acting during lithosphere breakup above a melting mantle: A case example in West Greenland: Tectonophysics, v. 581, p. 132–143, doi:10.1016/j.tecto.2011.11.020.

Ainsworth, N.R., Riley, L.A., Bailey, H.W., and Gueinn, J.J., 2014, Cretaceous–Tertiary Stratigraphy of the Labrador Shelf: St. John's, Riley Geoscience Limited for Nalcor Energy, 56 p.

Becker, K., Tanner, D.C., Franke, D., and Krawczyk, C.M., 2016, Fault-controlled lithospheric detachment of the volcanic southern South Atlantic rift: Geochemistry, Geophysics, Geosystems, v. 17, p. 887–894, doi:10.1002/2015GC006081.

Chalmers, J.A., and Laursen, K.H., 1995, Labrador Sea: The extent of continental and oceanic crust and the timing of the onset of seafloor spreading: Marine and Petroleum Geology, v. 12, p. 205–217, doi:10.1016/0264-8172(95)92840-S.

Chalmers, J.A., Larsen, L.M., and Pedersen, A.K., 1995, Widespread Palaeocene volcanism around the northern North Atlantic and Labrador Sea: Evidence for a large, hot, early plume head: Journal of the Geological Society [London], v. 152, p. 965–969, doi:10.1144/GSL.JGS.1995.152.01.14.

Chian, D., and Louden, K.E., 1994, The continent-ocean crustal transition across the southwest Greenland margin: Journal of Geophysical Research, v. 99, p. 9117–9135, doi:10.1029/93JB03404.

Chian, D., Keen, C., Reid, I., and Louden, K.E., 1995a, Evolution of nonvolcanic rifted margins: New results from the conjugate margins of the Labrador Sea: Geology, v. 23, p. 589–592, doi:10.1130/0091-7613(1995)023<0589:EONRMN>2.3.CO;2.

Chian, D., Louden, K.E., and Reid, I., 1995b, Crustal structure of the Labrador Sea conjugate margin and implications for the formation of nonvolcanic continental margins: Journal of Geophysical Research, v. 100, 24239, doi:10.1029/95JB02162.

Canada-Newfoundland and Labrador Offshore Petroleum Board, 2007, C-NLOPB Wells: St. John's, Newfoundland, Canada-Newfoundland and Labrador Offshore Petroleum Board: Schedule of Wells, http://www.cnlopb.ca/wells/.

Culshaw, N., Brown, T., Reynolds, P.H., and Ketchum, J.W.F., 2000, Kanairiktok shear zone: The boundary between the Paleoproterozoic Makkovik Province and the Archean Nain Province, Labrador, Canada: Canadian Journal of Earth Sciences, v. 37, p. 1245–1257, doi:10.1139/e00-035.

Deckart, K., Bertrand, H., and Liégeois, J.P., 2005, Geochemistry and Sr, Nd, Pb isotopic composition of the Central Atlantic Magmatic Province (CAMP) in Guyana and Guinea: Lithos, v. 82, p. 289–314, doi:10.1016/j.lithos.2004.09.023.

DeSilva, N.R., 1999, Sedimentary basins and petroleum systems offshore Newfoundland and Labrador, *in* Fleet, A.J., and Boldy, S.A.R., eds., Petroleum Geology of Northwest Europe: Proceedings of the 5th Conference on the Petroleum Geology of Northwest Europe: Geological Society of London Petroleum Geology Conference Series, v. 1, p. 501–516, doi:10.1144/0050501.

Divins, D., 2003, Total Sediment Thickness of the World's Oceans and Marginal Seas: Boulder, Colorado, National Oceanic and Atmospheric Administration National Geophysical Data Center, https://www.ngdc.noaa.gov/mgg/sedthick/sedthick.html.

Eldholm, O., and Sundvor, E., 1979, Geological events during the early formation of a passive margin: Tectonophysics, v. 59, p. 233–237, doi:10.1016/0040-1951(79)90047-7.

Etheridge, M.A., Symonds, P.A., and Lister, G.S., 1989, Application of the detachment model to reconstruction of conjugate passive margins, *in* Tankard, A.J., and Balkwill, H.R., eds., Extensional Tectonics and Stratigraphy of the North Atlantic Margins: American Association of Petroleum Geologists Memoir 46, p. 23–40, doi:10.1306/M46497C3.

Foley, S.F., 1989, Emplacement features of lamprophyre and carbonatitic lamprophyre dykes at Aillik Bay, Labrador: Geological Magazine, v. 126, p. 29–42, doi:10.1017/S0016756800006129.

Frei, D., Hutchison, M.T., Gerdes, A., and Heaman, L.M., 2008, Common-lead corrected U-Pb age dating of perovskite by laser ablation – magnetic sectorfield ICP-MS: 9th International Kimberlite Conference Extended Abstract, v. No. 9IKC-A, p. 1–3.

Funck, T., Louden, K.E., and Reid, I.D., 2001, Crustal structure of the Grenville Province in southeastern Labrador from refraction seismic data: Evidence for a high-velocity lower crustal wedge: Canadian Journal of Earth Sciences, v. 38, p. 1463–1478, doi:10.1139/e01-026.

Garde, A.A., Hamilton, M.A., Chadwick, B., Grocott, J., and McCaffrey, K.J.W., 2002, The Ketilidian orogen of South Greenland: Geochronology, tectonics, magmatism, and fore-arc accretion during Palaeoproterozoic oblique convergence: Canadian Journal of Earth Sciences, v. 39, p. 765–793, doi:10.1139/e02-026.

Geoffroy, L., 2001, The structure of volcanic margins: Some problematics from the North-Atlantic/Labrador-Baffin system: Marine and Petroleum Geology, v. 18, p. 463–469, doi:10.1016/S0264-8172(00)00073-8.

Geoffroy, L., 2005, Volcanic passive margins: Comptes Rendus Geoscience, v. 337, p. 1395–1408, doi:10.1016/j.crte.2005.10.006.

Haggart, J.W., 2014, New contributions in Baffin Bay/Labrador Sea petroleum exploration and development geoscience: Bulletin of Canadian Petroleum Geology, v. 62, p. 213–216, doi:10.2113/gscpgbull.62.4.213.

Hinchey, A.M., 2013, Geology of the Makkovik Area, Labrador (NTS 13O/03 and Parts of NTS 13O/02): Government of Newfoundland and Labrador, Department of Natural Resources Geological Survey Map 2013–07, Open File 013O/0138, scale 1:50000.

Holgate, N.E., Jackson, C.A.-L., Hampson, G.J., and Dreyer, T., 2015, Seismic stratigraphic analysis of the Middle Jurassic Krossfjord and Fensfjord formations, Troll oil and gas field, northern North Sea: Marine and Petroleum Geology, v. 68, p. 352–380, doi:10.1016/j.marpetgeo.2015.08.036.

Jauer, C.D., and Budkewitsch, P., 2010, Old marine seismic and new satellite radar data: Petroleum exploration of northwest Labrador Sea, Canada: Marine and Petroleum Geology, v. 27, p. 1379–1394, doi:10.1016/j.marpetgeo.2010.03.003.

Jauer, C.D., Oakey, G.N., Williams, G., Hans Wielens, J.B.W., and Haggart, J.W., 2014, Saglek Basin in the Labrador Sea, east coast Canada; stratigraphy, structure and petroleum systems: Bulletin of Canadian Petroleum Geology, v. 62, p. 232–260, doi:10.2113/gscpgbull.62.4.232.

Keen, C.E., Potter, P., and Srivastava, S.P., 1994, Deep seismic reflection data across the conjugate margins of the Labrador Sea: Canadian Journal of Earth Sciences, v. 31, p. 192–205, doi:10.1139/e94-016.

Kerr, A., Ryan, B., Gower, C.F., and Wardle, R.J., 1996, The Makkovik Province: Extension of the Ketilidian mobile belt in mainland North America, *in* Brewer, T.S., ed., Precambrian Crustal Evolution in the North Atlantic Region: Geological Society of London Special Publications 112, p. 155–177, doi:10.1144/GSL.SP.1996.112.01.09.

Kerr, A., Hall, J., Wardle, R.J., Gower, C.F., and Ryan, B., 1997, New reflections on the structure and evolution of the Makkovikian-Ketilidian orogen in Labrador and southern Greenland: Tectonics, v. 16, p. 942–965, doi:10.1029/97TC02286.

Ketchum, J.W., Culshaw, N.G., and Barr, S.M., 2002, Anatomy and orogenic history of a Paleoproterozoic accretionary belt: The Makkovik Province, Labrador, Canada: Canadian Journal of Earth Sciences, v. 39, p. 711–730, doi:10.1139/e01-099.

King, A.F., and McMillan, N.J., 1975, A Mid-Mesozoic breccia from the coast of Labrador: Canadian Journal of Earth Sciences, v. 12, p. 44–51, doi:10.1139/e75-005.

LaFlamme, C., Sylvester, P.J., Hinchey, A.M., and Davis, W.J., 2013, U-Pb age and Hf-isotope geochemistry of zircon from felsic volcanic rocks of the Paleoproterozoic Aillik Group, Makkovik Province, Labrador: Precambrian Research, v. 224, p. 129–142, doi:10.1016/j.precamres.2012.09.005.

Larsen, L.M., 2006, Mesozoic to Palaeogene Dyke Swarms in West Greenland and Their Significance for the Formation of the Labrador Sea and the Davis Strait: Geological Survey of Denmark and Greenland Report, 69 p.

Larsen, L.M., Rex, D.C., Watt, W.S., and Guise, P.G., 1999, ^{40}Ar-^{39}Ar dating of alkali basaltic dykes along the south-west coast of Greenland: Cretaceous and Tertiary igneous activity along the eastern margin of the Labrador Sea: Geology of Greenland Survey Bulletin, v. 184, p. 19–29.

Larsen, L.M., Heaman, L.M., Creaser, R.A., Duncan, R.A., Frei, R., and Hutchison, M., 2009, Tectonomagmatic events during stretching and basin formation in the Labrador Sea and the Davis Strait: Evidence from age and composition of Mesozoic to Palaeogene dyke swarms in West Greenland: Journal of the Geological Society [London], v. 166, p. 999–1012, doi:10.1144/0016-76492009-038.

Larsen, O., and Møller, J., 1968, K/Ar age determinations from western Greenlandl. Reconnaissance programme: Rapport Grønlands Geologiske Undersøgelse, v. 15, p. 82–86.

Latin, D., and White, N., 1990, Generating melt during lithospheric extension: Pure shear vs. simple shear: Geology, v. 18, p. 327–331, doi:10.1130/0091-7613(1990)018<0327:GMDLEP>2.3.CO;2.
Lavier, L.L., and Manatschal, G., 2006, A mechanism to thin the continental lithosphere at magma-poor margins: Nature, v. 440, p. 324–328, doi:10.1038/nature04608.
Leat, P.T., Thompson, R.N., Morrison, M.A., Hendry, G.L., and Dickin, A.P., 1990, Geochemistry of mafic lavas in the early Rio Grande Rift, Yarmony Mountain, Colorado, U.S.A.: Chemical Geology, v. 81, p. 23–43, doi:10.1016/0009-2541(90)90037-8.
Le Bas, M.J., 1989, Nephelinitic and basanitic rocks: Journal of Petrology, v. 30, p. 1299–1312, doi:10.1093/petrology/30.5.1299.
Le Bas, M.J., Le Maitre, R.W., Streckeisen, A., and Zanettin, B., 1986, A chemical classification of volcanic rocks based on the total alkali silica diagram: Journal of Petrology, v. 27, p. 745–750, doi:10.1093/petrology/27.3.745.
Lister, G.S., Etheridge, M.A., and Symonds, P.A., 1986, Detachment faulting and the evolution of passive continental margins: Reply: Geology, v. 14, p. 891–892, doi:10.1130/0091-7613(1986)14<891:CARODF>2.0.CO;2.
Martins, L.T., Madeira, J., Youbi, N., Munhá, J., Mata, J., and Kerrich, R., 2008, Rift-related magmatism of the Central Atlantic magmatic province in Algarve, southern Portugal: Lithos, v. 101, p. 102–124, doi:10.1016/j.lithos.2007.07.010.
McKenzie, D., 1978, Some remarks on the development of sedimentary basins: Earth and Planetary Science Letters, v. 40, p. 25–32, doi:10.1016/0012-821X(78)90071-7.
McWhae, J.R.H., Elie, R., Laughton, K.C., and Gunther, P.R., 1980, Stratigraphy and petroleum prospects of the Labrador Shelf: Bulletin of Canadian Petroleum Geology, v. 28, p. 460–488.
Peace, A., McCaffrey, K., Imber, J., Hobbs, R., van Hunen, J., and Gerdes, K., 2015, Quantifying the influence of sill intrusion on the thermal evolution of organic-rich sedimentary rocks in nonvolcanic passive margins: An example from ODP 210–1276, offshore Newfoundland, Canada: Basin Research, doi:10.1111/bre.12131.
Philippon, M., Willingshofer, E., Sokoutis, D., Corti, G., Sani, F., Bonini, M., and Cloetingh, S., 2015, Slip re-orientation in oblique rifts: Geology, v. 43, p. 147–150, doi:10.1130/G36208.1.
Ranero, C.R., and Pérez-Gussinyé, M., 2010, Sequential faulting explains the asymmetry and extension discrepancy of conjugate margins: Nature, v. 468, p. 294–299, doi:10.1038/nature09520.
Reid, I.D., and Keen, C.E., 1990, High seismic velocities associated with reflections from within the lower oceanic crust near the continental margin of eastern Canada: Earth and Planetary Science Letters, v. 99, p. 118–126, doi:10.1016/0012-821X(90)90075-9.
Rock, N.M.S., 1986, The nature and origin of ultramafic lamprophyres: Alnoites and allied rocks: Journal of Petrology, v. 27, p. 155–196, doi:10.1093/petrology/27.1.155.
Shallaly, N.A., Beier, C., Haase, K.M., and Hammed, M.S., 2013, Petrology and geochemistry of the Tertiary Suez rift volcanism, Sinai, Egypt: Journal of Volcanology and Geothermal Research, v. 267, p. 119–137, doi:10.1016/j.jvolgeores.2013.10.005.
Smith, W.H., and Sandwell, D., 1997, Global sea floor topography from satellite altimetry and ship depth soundings: Science, v. 277, p. 1956–1962, doi:10.1126/science.277.5334.1956.
Srivastava, S.P., 1978, Evolution of the Labrador Sea and its bearing on the early evolution of the North Atlantic: Geophysical Journal International, v. 52, p. 313–357, doi:10.1111/j.1365-246X.1978.tb04235.x.
Srivastava, S.P., and Roest, W.R., 1999, Extent of oceanic crust in the Labrador Sea: Marine and Petroleum Geology, v. 16, p. 65–84, doi:10.1016/S0264-8172(98)00041-5.
Shipboard Scientific Party, 1987, Site 646, *in* Srivastava, S.P., et al., Proceedings of the Ocean Drilling Program, Initial reports, Volume 105: College Station, Texas, Ocean Drilling Program, p. 419–674, doi:10.2973/odp.proc.ir.105.104.1987.
Storey, M., Duncan, R.A., Pedersen, A.K., Larsen, L.M., and Larsen, H.C., 1998, $^{40}Ar/^{39}Ar$ geochronology of the West Greenland Tertiary volcanic province: Earth and Planetary Science Letters, v. 160, p. 569–586, doi:10.1016/S0012-821X(98)00112-5.
Tappe, S., Foley, S.F., Jenner, G.A., Heaman, L.M., Kjarsgaard, B.A., Romer, R.L., Stracke, A., Joyce, N., and Hoefs, J., 2006, Genesis of ultramafic lamprophyres and carbonatites at Aillik Bay, Labrador: A consequence of incipient lithospheric thinning beneath the North Atlantic Craton: Journal of Petrology, v. 47, p. 1261–1315, doi:10.1093/petrology/egl008.
Tappe, S., Foley, S.F., Stracke, A., Romer, R.L., Kjarsgaard, B.A., Heaman, L.M., and Joyce, N., 2007, Craton reactivation on the Labrador Sea margins: $^{40}Ar/^{39}Ar$ age and Sr-Nd-Hf-Pb isotope constraints from alkaline and carbonatite intrusives: Earth and Planetary Science Letters, v. 256, p. 433–454, doi:10.1016/j.epsl.2007.01.036.
Tappe, S., Steenfelt, A., Heaman, L.M., and Simonetti, A., 2009, The newly discovered Jurassic Tikiusaaq carbonatite-aillikite occurrence, West Greenland, and some remarks on carbonatite-kimberlite relationships: Lithos, v. 112, p. 385–399, doi:10.1016/j.lithos.2009.03.002.
Torske, T., and Prestvik, T., 1991, Mesozoic detachment faulting between Greenland and Norway: Inferences from Jan Mayen fracture zone system and associated alkalic volcanic rocks: Geology, v. 19, p. 481–484, doi:10.1130/0091-7613(1991)019<0481:MDFBGA>2.3.CO;2.
Umpleby, D., 1979, Geology of the Labrador Shelf: Geological Survey of Canada Paper 79-13, 34 p.
Wardle, R.J., et al., 2002, Correlation chart of the Proterozoic assembly of the northeastern Canadian-Greenland Shield: Canadian Journal of Earth Sciences, v. 39, 895, doi:10.1139/e01-088.
Welford, J.K., and Hall, J., 2007, Crustal structure of the Newfoundland rifted continental margin from constrained 3-D gravity inversion: Geophysical Journal International, v. 171, p. 890–908, doi:10.1111/j.1365-246X.2007.03549.x.
Welford, J.K., and Hall, J., 2013, Lithospheric structure of the Labrador Sea from constrained 3-D gravity inversion: Geophysical Journal International, v. 195, p. 767–784, doi:10.1093/gji/ggt296.
Wernicke, B., 1985, Uniform-sense normal simple shear of the continental lithosphere: Canadian Journal of Earth Sciences, v. 22, p. 108–125, doi:10.1139/e85-009.
White, J.D.L., and Ross, P.S., 2011, Maar-diatreme volcanoes: A review: Journal of Volcanology and Geothermal Research, v. 201, p. 1–29, doi:10.1016/j.jvolgeores.2011.01.010.
White, R.S., 1992, Magmatism during and after continental break-up, *in* Storey, B.C., et al., eds., Magmatism and the Causes of Continental Break-up: Geological Society of London Special Publications 68, p. 1–16, doi:10.1144/GSL.SP.1992.068.01.01.
Whittaker, J.M., Goncharov, A., Williams, S.E., Müller, R.D., and Leitchenkov, G., 2013, Global sediment thickness data set updated for the Australian-Antarctic Southern Ocean: Geochemistry, Geophysics, Geosystems, v. 14, p. 3297–3305, doi:10.1002/ggge.20181.
Wilson, R.W., Klint, K.E.S., Van Gool, J.A.M., McCaffrey, K.J.W., Holdsworth, R.E., and Chalmers, J.A., 2006, Faults and fractures in central West Greenland: Onshore expression of continental break-up and sea-floor spreading in the Labrador–Baffin Bay Sea: Geological Survey of Denmark and Greenland Bulletin 11, p. 185–204, http://www.geus.dk/DK/publications/geol-survey-dk-gl-bull/11/Documents/nr11_p185-204.pdf.
Wilton, D.H.C., Taylor, R.C., Sylvester, P.J., and Penney, G.T., 2002, A review of kimberlitic and ultramafic lamprophyre intrusives from northern Labrador, *in* Current Research: Newfoundland Department of Mines and Energy Geological Survey Report 02-1, p. 343–352.
Woolley, A.R., Bergman, S.C., Edgar, A.D., Le Bas, M.J., Mitchell, R.H., Rock, N.M.S., and Scott Smith, B.H., 1996, Classification of lamprophyres, lamproites, kimberlites, and the kalsilitic, melilitic, and leucitic rocks: Canadian Mineralogist, v. 34, p. 175–186.